INFLUENCES ON CONIFER DROUGHT RESPONSES IN NORTHERN CALIFORNIA

By

Wallis Lee Robinson

A Thesis Presented to

The Faculty of Humboldt State University

In Partial Fulfillment of the Requirements for the Degree

Master of Science in Natural Resources: Forestry, Watershed, & Wildland Sciences

Committee Membership

Dr. Lucy Kerhoulas, Committee Chair

Dr. Rosemary Sherriff, Committee Member

Dr. Phil van Mantgem, Committee Member

Dr. Erin Kelly, Graduate Coordinator

July 2021

ABSTRACT

INFLUENCES ON CONIFER DROUGHT RESPONSES IN NORTHERN CALIFORNIA

Wallis Lee Robinson

California is experiencing increasingly severe and prolonged droughts, which are contributing to changes in tree stress and forest mortality. Many factors affect a tree's drought response, including competition, climate, and site and tree characteristics. Northern California provides a suitable venue to explore the effects of these factors, as it spans a variety of site conditions and includes habitat for conifers with different adaptations and requirements. This study used annual ^{13}C discrimination and growth metrics to assess differences in drought resistance and resilience in conifers adapted to coastal and montane ranges at both wet and dry sites, as well as differences in environmental factors that affect species-level drought responses. Coastal species (Sitka spruce and western hemlock) were more sensitive to drought than montane species (Shasta fir, Brewer spruce, sugar pine, and western white pine). Coastal trees were more sensitive to drought at dry sites than wet sites. Montane species exhibited smaller differences in drought resistance between wet and dry conditions, but varied in factors contributing to physiological response among species. This study suggests that in most situations, conifers in northern California weathered the 2012 – 2016 drought with reasonably high resistance and resilience. However, many of these trees may be at risk for increased stress and mortality in the event of longer and/or more frequent, severe

drought. Management strategies for conifers in one region may not be suitable for the same species in another region, and the effects of competition and community composition on drought resistance and resilience must be carefully considered.

ACKNOWLEDGEMENTS

This study was funded by the National Science Foundation (NSF GSS Award 1853903) and institutional support was provided by HSU's College of Natural Resource Science, College of Arts, Humanities, and Social Science, and Sponsored Programs Foundation (SPF). I would like to thank my committee members, Lucy Kerhoulas, Rosemary Sherriff, and Phil van Mantgem for their guidance and support. I would also like to thank Gabriel Roletti for sharing the field, lab, and logistical responsibilities for this joint graduate project with me, and for his intellectual contribution to the betterment of this project in the many conversations we've had sorting out various aspects of our respective studies.

Thanks to Erika Wright, Leslie Rodelander, and Kacie Flynn from SPF for their logistical and administrative support. Thanks to Kelly Muth for training me and others on tree core work and for her help, advice, and support in cross-dating cores. Thanks to Jill Beckman for her advice on statistical analysis and model selection. Thanks to Michael Kauffmann for study site recommendations and on-the-fly site replacement suggestions. Thanks to Adam Csank and Steve Leavitt for advice on isotope data and analysis. Thanks to Xiaoyu Zhang at the University of Arizona's Environmental Isotope Lab and Viorel Atudorei at the University of New Mexico's Center for Stable Isotopes for running stable isotope analyses for this project. Thanks to Michelle Dostal and Brandon Wilcox for access to work space in the Humboldt State University Chemistry Department. Thanks to Sean Fleming for his help in obtaining data during site selection. Thanks to Nicholas

Kerhoulas for help making tools to assist in tree corer maintenance in the field. Thanks to the many people in the National Park Service, California State Parks, the U.S. Forest Service, Humboldt Wildlife Refuge, and the City of Arcata who granted us access to study sites on land under their purvey. Finally, I would like to thank Sarah Aguiar, Perris Alfonzo, Sara Bandali, Asher Budnik, Ian Conway, Jeremy Dustin, Maeve Flynn, Gabriel Goff, Rosalio Gonzalez, Elizabeth Hinojosa, Sophia Lemmo, Suzanne Melendez, Diana Orozco, Brigitte Price, Ashley Shannon, and Colleen Smith for their incredible field and lab work over the course of this study; this project would not be possible without you.

TABLE OF CONTENTS

LIST OF TABLES

LIST OF FIGURES

LIST OF APPENDICES

INTRODUCTION

Drought is a major driver of the recent increase in tree mortality in the western United States (Allen et al., 2015). Drought also leads to increased water stress (Barber et al., 2000), wildfires (Crockett & Westerling, 2017), and susceptibility to bark beetle outbreaks (Ferrell et al., 1994), all of which contribute to widespread tree mortality. In California, droughts are projected to become more intense (Cook et al., 2015; Diffenbaugh et al., 2015; Grantham, 2018; Mastrandrea & Luers, 2012), which will likely exacerbate the effects on forests (Taylor & Guarin, 2005). California's 2012 – 2016 record-breaking drought fits within these predictions (D. Griffin & Anchukaitis, 2014), resulting in widespread tree mortality (Young et al., 2017) and intense wildfires (Crockett & Westerling, 2017). As such, the 2012 – 2016 drought provides an opportunity to assess the effects of severe, prolonged drought on forests of northern California as this region heads into another year (2021) of potentially severe to extreme drought (droughtmonitor.unl.edu, www.gov.ca.gov).

Northern California has not escaped the consequences of severe drought. In addition to the effects of the recent drought contributing to the deadly Camp and record-breaking Carr and Mendocino Complex fires, northern California is expected to continue experiencing severe drought in the future due to increasing temperatures and erratic precipitation (Grantham, 2018; Swain et al., 2018). Although the forests of northern California have significant carbon storage capacity (Hudiburg et al., 2009; Iberle et al.,

2020), enormous cultural significance (Baldy, 2013; Norgaard, 2014), and provide over 55% of the timber harvested in the state (McIver et al., 2015), research on drought in mixed conifer forests in California has largely centered on the central and southern Sierras (Bohner & Diez, 2021; Crockett & Westerling, 2017; Taylor & Guarin, 2005). Due to northern California's complex geography (DeCourten, 2009) and location at the intersection of several major bioregions (DellaSala et al., 1999; Grantham, 2018), research on Sierra Mountain forests may not be representative of drought response in forests of this region. To address the need for more region-specific information, this study used the 2012 – 2016 drought to evaluate the effects of a suite of environmental factors on conifer drought responses in northern California.

Factors Affecting Forest Response to Drought

Despite northern California's topographical heterogeneity, there are a few overarching geographical trends that are salient in studying forest responses to drought. Precipitation decreases to the south and east, while temperature increases along the same gradients (PRISM Climate Group, Oregon State University, https://prism.oregonstate.edu/, created 7 June 2021). These trends are further augmented by the presence of three mountain ranges (the Coast Range, Klamath Mountains, and the southern Cascades), which are subject to large amounts of winter precipitation at high

elevations and result in drier conditions to their east (Grantham, 2018). These trends combine to create two distinct environments: cool-wet coastal environments and seasonally hot-dry montane environments. Although a few conifer species grow both on the coast and in the mountains, most of the 36 conifer species throughout northern California grow primarily in one or the other of these two environments (J. R. Griffin, 1976; Kauffmann, 2012). In other regions, species adapted to wetter environments can be more sensitive to drought than those adapted to arid environments (e.g., Pompa-García et al., 2017). It is likely that this is also the case in northern California, where coastal species such as Sitka spruce (*Picea sitchensis* (Bong) Carr) and western hemlock (*Tsuga heterophylla* (Raf) Sarg) are adapted to more consistent water availability than montane species such as western white pine (*Pinus monticola* Douglas ex D. Don) and sugar pine (*Pinus lambertiana* Douglas; Niinemets & Valladares, 2006; Rueda et al., 2017).

Just as large-scale environmental factors can drive interspecific differences in drought response, local site characteristics may augment intraspecific differences in response, though the effects of some of these characteristics vary. Evidence from the Mediterranean and eastern United States indicates that most trees living in drier parts of their species' range are less resistant to drought than conspecific individuals living in wetter parts of their range (Adams & Kolb, 2004; Linares & Tiscar, 2010; Orwig & Abrams, 1997). Additionally, trees growing in relatively dry sites may have more short-term drought resistance, but suffer more significant growth reductions in the face of long-

term drought (Lévesque et al., 2013) compared to conspecific trees in relatively wet sites. However, some common garden experiments suggest that individuals sourced from dry environments are less drought resistant but recover and experience less mortality than conspecifics from wet environments (Chauvin et al., 2019; Isaac-Renton et al., 2018; Zas et al., 2020).

These apparent inconsistencies speak to the interaction of limiting factors in tree growth. Since trees are limited by combinations of temperature, light, and water availability (Nemani et al., 2003), there is not a straightforward answer to how an individual will react to changes in limiting factors. Trees limited by a combination of temperature, light, and/or water will likely have different responses to severe or prolonged drought depending on how the relevant limiting factors are affected (Lévesque et al., 2013; Nemani et al., 2003). Additionally, elevation, aspect, and slope can affect which of these resources are most limiting (Adams & Kolb, 2004; Linares & Tiscar, 2010; Primicia et al., 2015). The complex topography of northern California therefore complicates prediction of drought response.

Competition can also limit a tree's access to resources and be an important factor in drought response and mortality (Young et al., 2017). Shifts in fire regimes related to the attempted genocide of indigenous people in California (Bacon, 2019; Fenelon & Trafzer, 2014; Cowan, 2019) and subsequent settler-colonial land management (i.e., logging, fire exclusion, and grazing) have dramatically changed the stand structure of

many forests in this region (Knapp et al., 2013; Norman & Taylor, 2005). Fire exclusion in particular has resulted in denser stands with less fire-resistant trees and high fuel loads in many forests (Taylor, 2000). Though species composition and increased fuel loads are directly linked to more intense wildfires (Naficy et al., 2010), stand density also affects tree mortality (Taylor & Guarin, 2005). Denser stands may result in more rapid spread of disease (Parker et al., 2006) and bark beetle outbreaks (Fettig et al., 2007), as well as more competition for resources, which slows tree growth even in non-drought circumstances (Das, 2012). These structural changes are important to consider when studying the effects of severe drought on conifer forests.

Many taxa display positive correlations between range size and ecological breadth, particularly between range size and tolerance of climatic variation (Morin & Chuine, 2006; Slatyer et al., 2013). This pattern suggests that changes in climatic factors associated with drought should affect species with small range sizes more than those with larger ranges. The few studies comparing drought response across species with different range sizes indicate that conifers with smaller range size are more at risk for low drought resistance (Lévesque et al., 2013). Given that northern California is home to 36 conifer species, several of which are at the southern edge of their range or are restricted to the region (DellaSala et al., 1999; Kauffmann, 2012), this is an ideal area to assess drought response in conifers with different adaptations and requirements.

This study used a combination of growth and stable carbon isotope analyses to evaluate the effects of the 2012 – 2016 drought on six conifer species across northern California. Specifically, this study aimed to answer the following questions: 1) How does drought resistance during prolonged drought differ between species occupying coastal and montane ranges? 2) Within coastal and montane ranges, how does drought resistance during prolonged drought differ between wet and dry habitats? And 3) how do competition, climate, and site and tree characteristics influence tree physiology (as measured by ^{13}C discrimination) by species? The answers to these questions have important regional conservation and management implications, and will aid in preparing for a climate-uncertain future.

Measurements of Forest Drought Response

Ring-width and stable carbon isotope measurements are commonly used to evaluate drought response (e.g., Barber et al., 2000; Lévesque et al., 2013; Sohn et al., 2013). Radial growth alone is not always a reliable indicator of a tree's drought response, since water-stressed trees may allocate more resources to root development (Eziz et al., 2017; Klein et al., 2011) and/or depend more heavily on carbon reserves (Dickman et al., 2015). Thus, using only growth-based drought resistance (during drought/pre-drought ratio) and resilience (post-drought/pre-drought ratio) can over- or under-estimate drought

response due to uncertainty regarding changes in resource allocation. Additionally, drought resistance and resilience, as quantified in this way, are influenced by how the pre-drought period is defined, so there are limitations to this approach (Schwarz et al., 2020).

While radial growth is dependent on resource availability and allocation, the degree to which the enzyme Rubisco discriminates against ^{13}C in favor of ^{12}C during carbon fixation is partially dependent on water stress, which allows ^{13}C discrimination ($\Delta^{13}C$) to be used as an important proxy for drought response. When a plant is water-stressed, it closes its stomata, decreasing both transpirational water loss and CO_2 uptake. This results in the incorporation of more ^{13}C into the wood made during years associated with water stress (McCarroll & Loader, 2004). Contrastingly, the amount of ^{13}C in wood also decreases with photosynthetic rate due to decreased CO_2 demand (Farquhar et al., 1989; McCarroll & Loader, 2004). Therefore, if stomatal conductance decreases, but photosynthetic rate decreases at the same time, the two mechanisms can "cancel out," resulting in similar $\Delta^{13}C$ under different physiological circumstances. Thus, the use of both isotope- and growth-based indices can highlight temporal differences between physiological and growth responses to drought and improve understanding of potential mechanisms driving drought responses.

2. MATERIALS AND METHODS

2.1 Study Area

Study sites were located across three biogeographic regions in northern California: the Klamath Mountains, the southern Cascades, and the North Coast (Cleland, 2007, Figure 1). These regions cover land in relationship with many indigenous communities including the Pomo, Mattole, Wiyot, Karuk, Hupa, Yurok, Tolowa Dee-ni', Lassik, Wintu, Shasta, Modoc, and Maidu tribes (*Northern California Indian Development Council*, 2021). Collectively, these regions sit at the intersection of the Cascades, the Modoc Plateau and Great Basin, and the California central valley. These three regions vary in geologic history, with the Klamath Mountains bearing the oldest formations, followed by the North Coast and southern Cascades. The Klamath Mountains and North Coast both contain a complex mixture of metamorphic bedrock (mostly of the Franciscan complex in the North Coast) interrupted by serpentinite and other silica-rich formations, while the southern Cascades are characterized by a series of young volcanos and the resulting extrusive formations (DeCourten, 2009). While the North Coast is predominated by rich, alluvial soils, the Klamath Mountains contain primarily gravelly, moderately- to well-drained loamy soil with pockets of soils derived from ultramafic bedrock such as serpentinite (Skinner et al., 2006), and the southern Cascades contain gravelly, moderately- to well-drained volcanic soils (Skinner & Taylor, 2006).

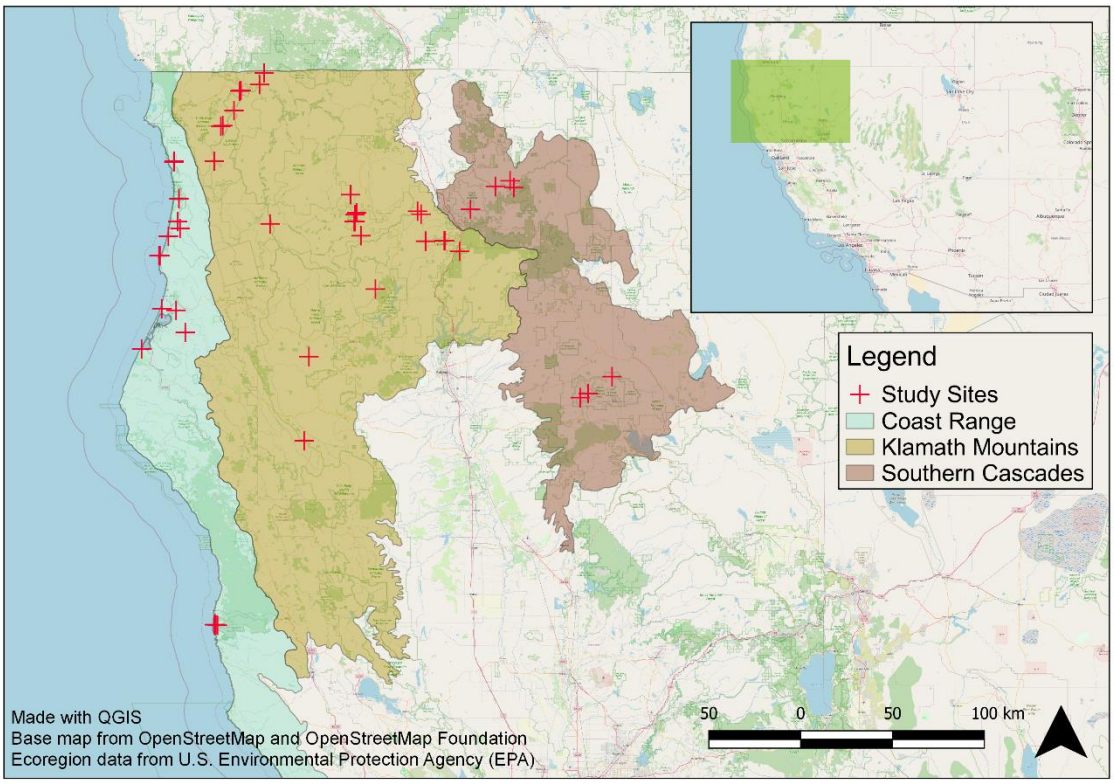

Figure 1. Map of the study area. Red plus signs denote the locations of study sites across northern California. Map made with QGIS (QGIS Development Team, 2021) using level III ecoregion data from the U.S. Environmental Protection Agency (*Level III Ecoregions of the Continental United States*, 2013).

The climate of the North Coast is typically cool and humid year-round, while the Klamath Mountains and southern Cascades experience warm, dry summers and cool, wet winters. The 30-year average minimum winter temperature ranges from 5 °C along the coast to -6 °C in the montane regions, and the maximum summer temperature from 20 °C on the coast to 27 °C in montane regions (PRISM Climate Group, Oregon State University, https://prism.oregonstate.edu/, created 7 June 2021). From south to north, 30-

year average (1981 – 2010) annual precipitation increases from 1,151 mm to 1,924 mm along the coast, and from 1,278 mm to 2,012 mm in montane regions. However, during recent years (including the 2007 – 2016 study period), coastal regions have experienced more precipitation than montane regions, primarily due to a decrease in winter precipitation in the latter (Appendix A).

2.2 Site Selection

The taxa of interest included two montane species with restricted ranges and local abundance, Brewer spruce (*Picea breweriana* S. Watson) and Shasta fir (*Abies magnifica* var. *shastensis* Lemmon), two montane species in the middle of their widespread ranges, sugar pine and western white pine, and two coastal species at the southern border of their widespread ranges, Sitka spruce and western hemlock (Table 1). Sitka spruce and western hemlock occur in low elevation, wet, coastal habitats, while the other four species occur in seasonally-dry montane habitats at mid to high elevations.

Table 1. Number of trees per species, mean (± 1 SE) diameter at breast height (DBH), total Hegyi index, annual basal area increment (BAI), and ^{13}C discrimination ($\Delta^{13}C$) from 2007 to 2016 for each focal species.

Species	**Trees**	**DBH (cm)**	**Hegyi**	**BAI (cm^2)**	**$\Delta^{13}C$ (‰)**
Coastal					
Sitka spruce	44	110 ± 7	1.0 ± 0.1	115 ± 3	19.8 ± 0.1
Western hemlock	31	85 ± 5	1.2 ± 0.2	51 ± 3	19.1 ± 0.1
Montane					
Shasta fir	45	83 ± 4	1.9 ± 0.2	31 ± 1	18.3 ± 0.0
Brewer spruce	45	57 ± 3	2.3 ± 0.3	23 ± 1	17.5 ± 0.0
Sugar pine	45	90 ± 3	1.4 ± 0.2	31 ± 1	18.1 ± 0.0
Western white pine	45	77 ± 4	1.5 ± 0.2	22 ± 1	17.0 ± 0.0

Potential sites for each of the six conifer species within northern California were obtained from observational data on Calflora (http://calflora.org) and supplemented when needed with suggestions by a local expert (Michael Kauffmann, pers. comm). Locations with greater than 30% slope, greater than 3.2 km from a road, and with evidence of fire (CalFire database) or harvesting (Google Earth) were excluded. Since annual precipitation is a major driver of local climate effects on drought response (Young et al., 2017), potential sites for each species were sorted using 30-year average (1981 – 2010) annual precipitation data obtained at a four-kilometer resolution from PRISM Climate Group. These 30-year average precipitation values were ranked into low, middle, and high categories for each species, and labeled as dry, moderate, and wet sites, respectively (Appendix Table A1). Three sites in each precipitation category with the lowest 2014 (a notably dry year) Palmer Drought Severity Index (PDSI) values were selected as study

sites (9 sites total per species). Additional factors including elevation, soil type (serpentine or not), and other site factors were also taken into account during analysis.

2.3 Field Methods

Data were collected in 2019 and 2020. All sites were accessed by driving to the trailhead or road closest to a site's GPS point. A site was defined as the 3.2 km radius surrounding the GPS point of the site location from Calflora. Within each site, the closest 10 canopy dominant or co-dominant focal trees for each species that met our criteria (see below) were non-randomly selected for coring and data collection, resulting in 540 trees sampled for cross-dating purposes. However, only the first five trees at each site were used for isotope analysis, resulting in 270 trees. As possible, focal trees were selected to capture a wide range of competitive environments within a site.

Focal trees were at least 20 m from any road, 10 m from any trail, and 15 m away from any bodies of water. In addition, trees near seeps and disturbed areas were avoided. Focal trees were without major injuries, co-dominant or dominant in the surrounding canopy, and more than 20 m away from any other focal tree when possible. A few intermediate trees were measured for western hemlock, Sitka spruce, and Brewer spruce in situations where there were not enough appropriate trees of the target canopy class.

Once a tree was selected, two cores were taken at a 90º angle from one another. For the first five trees, one of the two cores was a 12 mm core for isotopic analysis. Each core had at least 50 rings to ensure accurate cross-dating. For each core location on the bole, height, tree diameter, and bark thickness were recorded to calculate basal area increment (BAI).

In addition to tree cores, the following information was recorded for each focal tree: GPS location, crown class (dominant, co-dominant, or intermediate), crown ratio (crown length/tree height), diameter at breast height (1.37 m, DBH), and local competition. To measure local competition around each focal tree, the following information was recorded for all neighboring trees with a DBH greater than 5 cm within a 10 m radius: DBH, species, and distance from focal tree. This information was then used to calculate competition indices (see below). Particularly dominant understory shrubs were also noted if present and were included in competition indices if they possessed stems with a diameter greater than 5 cm DBH.

2.4 Selection of Study Years

The recent California drought is typically considered to have lasted from 2012 to 2016. However, 2012 was not a particularly dry year in northern California; PDSI values were uniformly greater than -2 in 2012 across all sites in this study (Figure 2a). For this

reason, the five-year pre-drought period was defined as 2008 – 2012. Similarly, 2016 was not a notably dry year for most study sites (average of -0.9 ± 0.0 PDSI across all sites; Figure 2a). However, 2016 was included in analyses to evaluate for a possible delayed drought response or drought resilience.

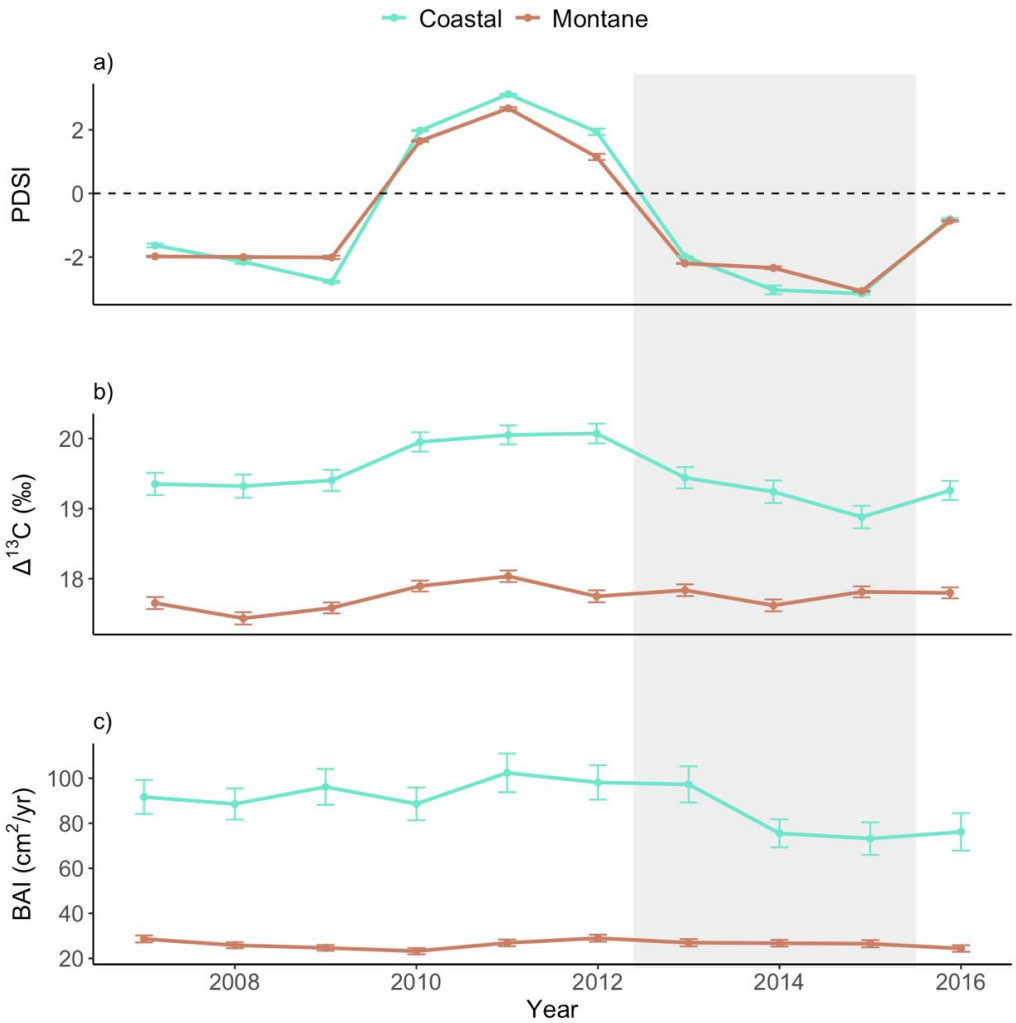

Figure 2. Mean (± SE) a) Palmer Drought Severity Index (PDSI) values, b) ^{13}C discrimination ($\Delta^{13}C$), and c) annual basal area increment (BAI) across all study sites (n = 53) between 2007 and 2016. Study sites are divided into coastal and montane categories. Drought period (2013 – 2015) is shaded grey.

2.5 Lab Methods

Core and Isotope Sample Preparation

Cores were mounted and sanded on a belt sander or by hand to ensure sufficient material for isotope analysis. Cores were then scanned at 1200 dpi (dots per inch) into the WinDendro program (Régent Instruments Inc., Québec, Canada) for measurement following the Dendroecology Lab procedure (K. Muth, pers. comm., October, 2019). If tree-rings were too narrow to reliably discern from scans, a binocular dissecting microscope was used to review the core. The resulting tree-ring series were cross-dated using the COFECHA program (Holmes, 1984). Each tree core was cross-dated as far back in time as possible so that the chronology may be used in future studies.

Individual rings were excised for six pre-drought years (2007 – 2012, although 2007 was a dry year, so only 2008 – 2012 were used for calculating the pre-drought average), three drought years (2013 – 2015), and one post-drought year (2016) for isotope analysis. To save material and time, most of these rings were not milled. Historically, samples were milled to ensure complete combustion during mass spectrometry. Given current technology, full combustion happens regardless of whether milling is done or not, and produces similar results (L. Kerhoulas, pers. comm., October 2019; S. Leavitt, pers. comm., November 2019; H. Zald, unpublished results, December 2019). However, since this is not yet a widely accepted practice, a small number of rings (n = 68) from study cores taken from a subset of focal trees (n = 23) were selected to

compare the mass spectrometry results from milled and unmilled samples of the same ring. Target weights for milled and unmilled samples were 0.5 mg and 0.8 to 1.2 mg, respectively (L. Kerhoulas, pers. comm., March 2020). Whole wood was used for isotope analysis since there is no notable difference in isotope trends from whole wood and cellulose samples (Borella et al., 1998). Rings for the pilot study comparing milled and unmilled samples were sent to the Center for Stable Isotopes at the University of New Mexico for analysis on a Thermo Finnigan Delta V isotope ratio mass spectrometer (IRMS; Thermo Scientific, Waltham, MA, USA) connected to a Costech elemental analyzer (EA; Costech Analytical, Valencia, CA, USA). All other rings were sent to the stable isotope lab at the University of Arizona for analysis on a Finnigan Delta PlusXL IRMS (Thermo Scientific, Waltham, MA, USA) connected to a Costech EA (Costech Analytical, Valencia, CA, USA) with an analytical precision of ± 0.1‰. This analysis found strong correlation between milled and unmilled samples (R^2 = 0.96; Figure 3), thereby supporting the use of unmilled samples for the rest of the study.

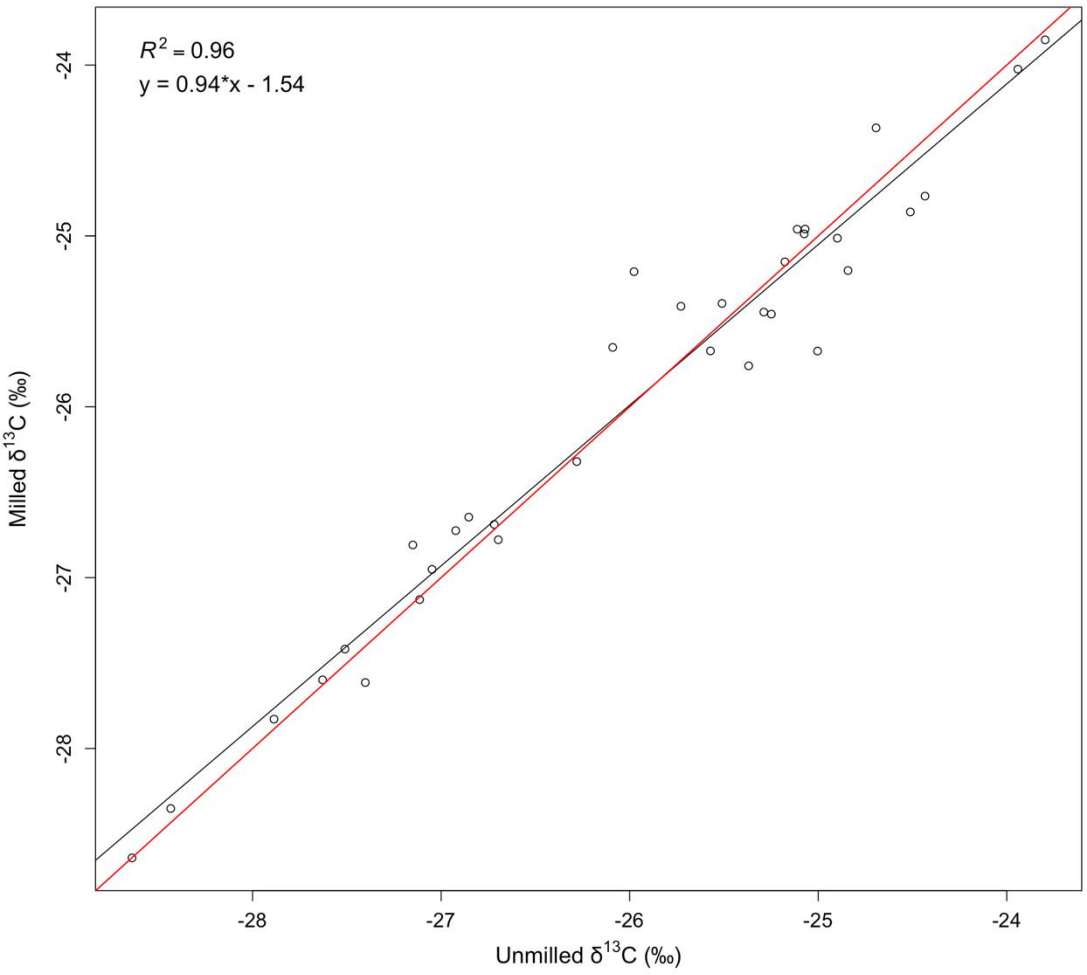

Figure 3. Correlation plot of carbon stable isotope ratios ($\delta^{13}C$) in unmilled tree-rings compared to paired milled tree-rings (n = 68 tree-rings from 23 trees). The 1:1 line is shown in red. Multiple $R^2 = 0.96$, $p < 0.001$.

Calculation of Response Variables

All $\delta^{13}C$ values were converted to ^{13}C discrimination using the following equation (Farquhar et al., 1989):

$$\Delta^{13}C = (\delta^{13}C_{air} - \delta^{13}C_{plant})/(1 + \delta^{13}C_{plant}/1000) \quad (1)$$

where $\Delta^{13}C$ is ^{13}C discrimination, $\delta^{13}C_{plant}$ is the tree-ring $\delta^{13}C$ from the mass spectrometer, and $\delta^{13}C_{air}$ is the isotopic signature of the $\delta^{13}C$ of the air during the year corresponding to the year of formation of the tree-ring, using atmospheric data from the Scripps CO_2 Program's La Jolla sampling station (2007 – 2016; Keeling et al., 2005, McCarroll & Loader, 2004; White & Vaughn, 2011). Note that this means that although $\delta^{13}C$ values increase with stomatal closure, $\Delta^{13}C$ decreases with stomatal closure (less CO_2 availability, so less discrimination by RuBisco).

To assess tree growth, BAI was calculated using the dplR package in R with the assumption that the cross-section of each tree is circular using the following equation (Biondi & Qeadan, 2008; Bunn et al., 2018):

$$BAI_t = \pi (R_o - \sum_o^t \omega)^2 - \pi (R_o - \sum_o^{t-1} \omega)^2 \quad (2)$$

where R_o is the radius of the tree, obtained by halving the DBH and subtracting the average bark thickness, t is the year for which BAI is being calculated, and ω is the average ring-width for a given year.

Isotope-based and growth-based drought resistance were calculated using the following equations:

$$DR_{13C} = \Delta^{13}C_{dd}/\Delta^{13}C_{pd} \quad (3)$$

$$DR_{BAI} = BAI_{dd}/BAI_{pd} \quad (4)$$

where DR_{13C} and DR_{BAI} represent isotope- and growth-based drought resistance, respectively, the dd subscript represents the $\Delta^{13}C$ or BAI value during a single drought year or the average of multiple drought years, and the pd subscript denotes the average of the five years (2008 – 2012 in this case) prior to the drought. Note that isotope-based drought resistance values closer to one generally indicate less stomatal sensitivity to drought (less stomatal regulation), while values less than one indicate more stomatal sensitivity. Values more than one likely represent either stochastic tree-level events or a decrease in a tree's photosynthetic capacity. Growth-based drought resistance at or above one also represents low drought sensitivity and/or stochastic tree-level events, while values lower than one likely indicate either reduced photosynthetic capacity or reduced allocation of carbon toward radial growth.

Competition Data

Data from competitor trees within 10 m of each focal tree were used to calculate the Hegyi competition index and a variation of the Hegyi index, as well as trees per hectare (TPH). The Hegyi index was calculated using all live competitor trees with the following equation (Canham et al., 2004; Hegyi, 1974):

$$CI_i = \sum_{j=1}^{n} \left(\frac{DBH_j \div DBH_i}{dist_{ij}}\right) \quad (5)$$

where CI_i is the competition index for the focal tree, DBH_j is the diameter of the competitor tree, DBH_i is the diameter of the focal tree, and $dist_{ij}$ is the distance between

the focal tree and the competitor tree. The variation on the Hegyi competition index is a conspecific Hegyi ratio, which is obtained by dividing a tree's intraspecific Hegyi index by its total Hegyi index. Unlike the Hegyi index, which measures absolute competition levels, conspecific Hegyi ratio is a relative measure of type of competition. This allows for the proportion of intraspecific to interspecific competition to be considered.

Since the Hegyi index gives more weight to large or close competitor trees, smaller trees that make up a large component of the understory do not have as strong an influence on Hegyi indices as larger trees. Small trees were therefore better captured by TPH, which relies solely on the number of individuals per species present per plot. The TPH for each focal tree was calculated by summing the number of competitor trees within the 10 m radius of each focal tree and then scaling from trees per plot to trees per hectare.

Drought and Climate Data

I used site-specific values of annual water-year precipitation (PPT_{wy}, i.e., the precipitation from the previous October through the current September), 30-year average precipitation (1981 – 2010, i.e., long-term moisture conditions), maximum annual temperature (T_{max}), and minimum annual temperature (T_{min}, which may be correlated with length of growing season), instead of a single term such as PDSI or climatic water deficit to evaluate the influence of both moisture and temperature on tree response. All

climate data except for 30-year precipitation averages were obtained as monthly values from the TerraClimate database (http://www.climatologylab.org/terraclimate.html) using the coordinates from the first focal tree at each site. Thirty-year precipitation data were obtained from the PRISM Climate Group since this was the source used to obtain this information for site selection. Data from both sources were obtained at a four-kilometer resolution.

Site Characteristics

To account for topographic and soil differences among sites, heat load index (HLI), elevation, and soil type (serpentine or not) were assessed for significance in the $\Delta^{13}C$ models. Heat load index data were obtained from the R package spatialEco (McCune & Keon, 2002), elevation data were obtained from the USGS National Elevation Dataset program (https://viewer.nationalmap.gov/basic/), and soil data were derived from USGS geologic data (D. Burge and S. Harrison, 2016 unpublished data).

2.6 Statistical Analysis

Drought Resistance and Resilience Across Range Type and Site Condition

To answer the first two questions of this study, isotope- and growth-based drought resistance and resilience values were calculated for each drought and post-drought year for coastal and montane species (Question one) and for wet and dry sites within coastal

and montane species (Question two). All analyses with isotope-based and growth-based drought resistance (2013 – 2015) and resilience (2016) used the same trees.

Annual isotope- and growth-based drought resistance and resilience were assessed using a linear mixed-effects model with range type (coastal or montane) and year as predictors. Since these models included multiple (annual) drought resistance values per tree, the random effect for both of these models was trees nested in site. A 2-way ANOVA was used to determine whether drought resistance differed significantly by species range and/or year for each model. Specific differences in average drought resistance between each species were elucidated using Tukey's multiple comparison test (packages emmeans and multicomp in R; Hothorn & Bretz, 2008; Lenth, 2021). Species-level drought resistance and resilience models were also created for all six species, as well as for all species within each range type, and evaluated in the same way as the annual range type model (Appendix B).

Mean isotope- and growth-based drought resistance values were also calculated by species across the three drought years (2013 – 2015). Both measures of mean drought resistance were assessed in linear mixed-effects models with species as the only predictor with a random effect of site. An ANOVA was used to determine whether average drought resistance differed significantly by species. Specific differences were identified by using Tukey's multiple comparison test. This assessed differences in overall drought resistance between range types for the entire drought period, and also whether species had more

similar drought resistance values within each range type than between range types. This was important since modeling drought resistance and resilience for all six species at an annual resolution resulted in high levels of collinearity (but see Appendix B).

To evaluate whether local site characteristics augment intraspecific differences in drought response, the two wettest and driest (30-year average precipitation) sites, per species, at least half a standard deviation away from the mean were categorized as wet or dry habitats, respectively. Only one wet Shasta fir site was included because no other Shasta fir sites were half a standard deviation wetter than the species mean. The significance of year and habitat was evaluated separately for coastal and montane species by modeling annual isotope- and growth-based drought resistance for each species range (coastal and montane) in linear mixed-effects models with habitat (wet or dry) and year as predictors and a random effect of trees nested in site. These models were then evaluated using the same methods employed to test for differences in annual drought resistance between coastal and montane species. All models were evaluated for normality of residuals and log-transformed if necessary to meet this requirement.

Investigating Species-Level Physiology via ^{13}Carbon Discrimination

The effects of drought, competition, climate, site and tree characteristics on annual $\Delta^{13}C$ were determined using linear mixed-effects models with the nlme package in R (Pinheiro et al., 2018). Models included data from all ten study years (2007 – 2016).

Six species-specific models were developed, which included a random intercept with random effects of tree nested in site to account for non-independence in site- and tree-level observations. In addition to these six models, two range-level models were also made to assess the most important factors affecting $\Delta^{13}C$ in coastal species (Sitka spruce and western hemlock) and montane species (Shasta fir, Brewer spruce, sugar pine, and western white pine). This approach allowed for assessment of trees with similar $\Delta^{13}C$ values using a larger sample size, but also presented the risk of erroneously extrapolating results driven by one species across multiple species. Thus, species was included as an additional predictor variable during model selection. Pooled models were only considered useful if predicted $\Delta^{13}C$ means for each species were similar to measured means.

Each potential predictor variable fit into one of four categories (competition, drought and climate metrics, site, or tree-level characteristics; see Appendix C). Each variable was first assessed individually to determine if a model with the given variable was better at predicting $\Delta^{13}C$ than a model fitted with only the intercept. All variables with greater predictive power than the intercept were then evaluated in a global model. The model that maintained an Akaike Information Criterion for small sample sizes (AICc) of at least two less than the model with the next fewest terms was selected. All reasonable interaction terms (Table 2, Appendix C) were evaluated after this initial variable selection and held to the same standards of parsimony. Models were then evaluated for first and second order autocorrelation terms (AR1 and AR2) to account for

potential correlation in $\Delta^{13}C$ across years. The autocorrelation structure with the lowest AICc by at least two was used for the final model. Depending on the species, the best autocorrelation structure ranged from none to a second-order autocorrelation structure. All combinations of the global model were also tested with the best autocorrelation structure as a final check for each species. Final model terms were then evaluated for significance and collinearity. Backward selection was used to eliminate terms with a *p*-value > 0.05 using a likelihood ratio test, and models were not accepted if they had variable inflation factors greater than 2.

Table 2. Interactions tested in model selection. Potential interacting terms include total Hegyi index (CI), conspecific Hegyi ratio (CI_{cs}), trees per hectare (TPH), water-year precipitation (PPT_{wy}), annual maximum and minimum temperature (T_{max} and T_{min}), 30-year precipitation average (PPT_{30}), heat load index (HLI), and DBH.

Interaction	Justification
CI x PPT_{wy}	More competition could result in stomatal closure to conserve water overall, (lower $\Delta^{13}C$) but could also result in lower evapotranspirational demand during drought (more competition → lower $\Delta^{13}C$ and less variation in $\Delta^{13}C$)
CI x T_{max}	More competition could result in stomatal closure to conserve water (lower $\Delta^{13}C$), but could also provide a temperature buffer during drought (more competition → lower $\Delta^{13}C$ and less variation in $\Delta^{13}C$)
CI x T_{min}	Longer growing season with high competition → faster depletion of available water → lower $\Delta^{13}C$
CI x DBH	Big trees in competitive environments may be under greater hydraulic stress than in less competitive environments
CI_{cs} x T_{min}	Longer growing season with high intraspecific resource competition → faster depletion of available water → lower $\Delta^{13}C$
CI_{cs} x DBH	Big trees in competitive environments may be under greater hydraulic stress than in less competitive environments, especially if competing with conspecifics
TPH x PPT_{wy}	More competition could result in stomatal closure to conserve water overall, (lower $\Delta^{13}C$) but could also result in lower evapotranspirational demand during drought (more competition → lower $\Delta^{13}C$ and less variation in $\Delta^{13}C$)
TPH x T_{max}	More competition could result in stomatal closure to conserve water (lower $\Delta^{13}C$), but could also provide a temperature buffer during drought (more competition → lower $\Delta^{13}C$ and less variation in $\Delta^{13}C$)
TPH x T_{min}	Longer growing season with high competition → faster depletion of available water → lower $\Delta^{13}C$
TPH x DBH	Big trees in competitive environments may be under greater hydraulic stress than in less competitive environments
PPT_{30} x PPT_{wy}	Trees growing in dry places may be more acclimated to drought or more sensitive to drought
PPT_{30} x T_{max}	Trees growing in dry places may be more acclimated to drought or more sensitive to drought
HLI x PPT_{wy}	Higher HLI could result in more stomatal conductance during wet conditions but more stomatal closure with high evapotranspirational demand
HLI x DBH	Greater HLI could have different effects on big and smaller trees depending on light environment
DBH x PPT_{wy}	Larger size could result in more hydraulic stress (lower $\Delta^{13}C$) or greater access to deeper water sources (higher $\Delta^{13}C$)
DBH x T_{max}	Larger size could result in more hydraulic stress (lower $\Delta^{13}C$) or greater access to deeper water sources (higher $\Delta^{13}C$)

3. RESULTS

3.1 Drought Resistance in Coastal and Montane Conifer Species in Northern California

Coastal species had marginally to significantly lower average isotope- and growth-based drought resistance than montane species (Table 3, Figure 4). In contrast, average isotope- and growth-based drought resistance did not significantly differ between species within each range type. The model for species-level differences suffered from high collinearity and was split into range-level (coastal and montane) models. However, both the species-level and range-level models showed that species within the same range type had similar annual drought resistance, with a few exceptions (Appendix B).

Table 3. Summary of mean (± SE) isotope- and growth-based drought resistance (DR) during the drought (2013 – 2015) by species.

Site	Isotope DR	Growth DR
Coastal		
Sitka spruce	0.97 ± 0.01	0.86 ± 0.04
Western hemlock	0.97 ± 0.01	0.83 ± 0.04
Montane		
Shasta fir	1.00 ± 0.01	0.99 ± 0.04
Brewer spruce	1.01 ± 0.01	1.01 ± 0.05
Sugar pine	1.00 ± 0.01	1.05 ± 0.05
Western white pine	1.00 ± 0.01	0.97 ± 0.04

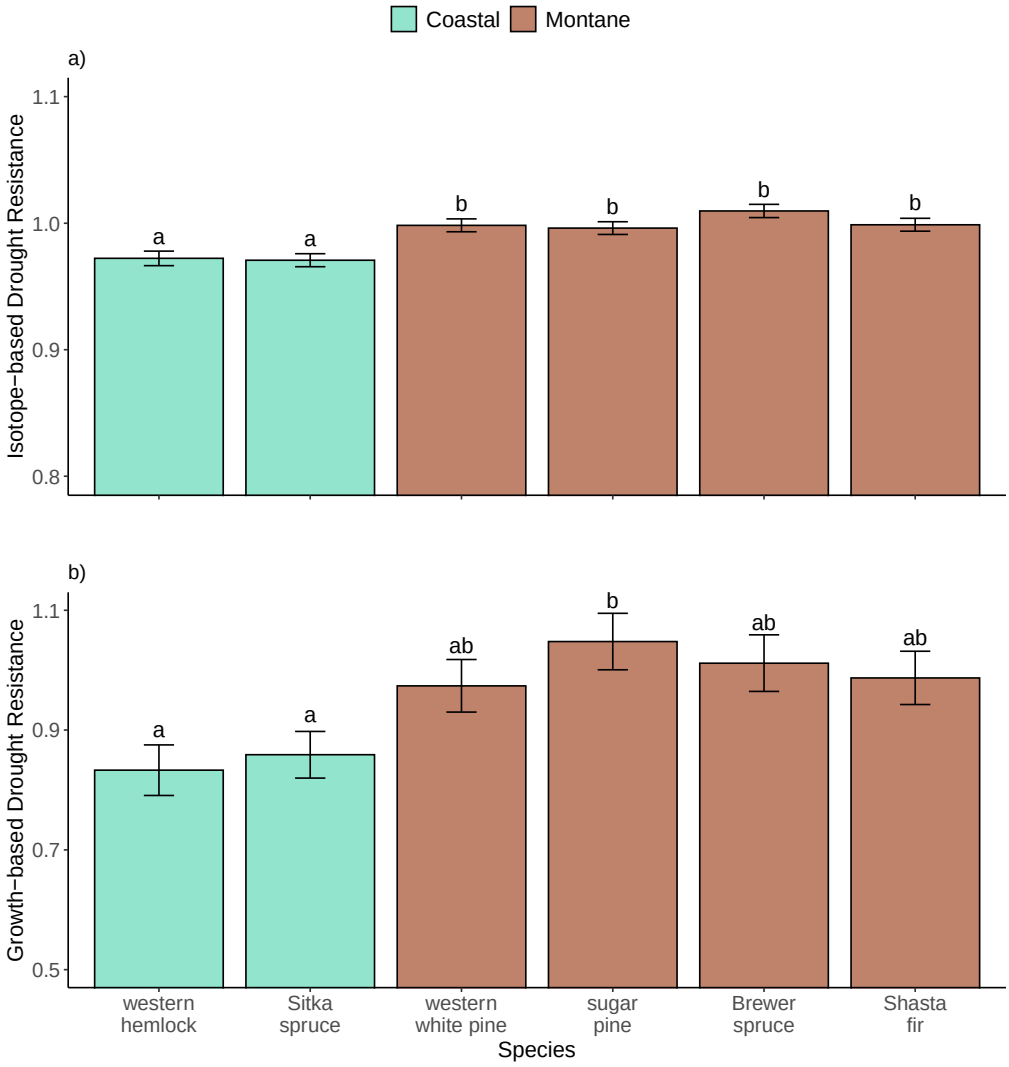

Figure 4. Mean (± SE) a) isotope-based drought resistance and b) growth-based drought resistance during the drought (2013 – 2015) by species (n = 255 trees). Different letters represent significant ($p < 0.05$) differences among species. Note that the y-axis extends from 0.80 to 1.10 in a) and from 0.50 to 1.10 in b).

Coastal species experienced a significant decline in isotope-based drought resistance with each successive year of drought, but also exhibited high resilience in 2016, with $\Delta^{13}C$ levels similar to 2014 (Table 4, Figure 5a). Growth-based drought

resistance in coastal species similarly declined through 2015, but showed lower resilience than isotope-based measurements in 2016 (Table 4, Figure 5b). Montane species maintained higher levels of isotope- and growth-based drought resistance relative to coastal species under similar drought severity conditions (see PDSI values in Figure 5). Although montane species experienced a significant decline in isotope-based drought resistance in 2014, $\Delta^{13}C$ rebounded to 2013 levels in 2015 and remained stable through 2016 (Table 4, Figure 5a). In contrast, growth-based drought resistance in montane species experienced a two-year lag relative to isotope-based drought resistance, with BAI only decreasing in 2016 (Table 4, Figure 5b).

Table 4. Summary of mean (± SE) annual isotope- and growth-based drought resistance and 2016 resilience for coastal and montane species.

Site	**Isotope Response** (Resistance 2013 – 2016) (Resilience 2016)	**Growth Response** (Resistance 2013 – 2016) (Resilience 2016)
Coastal		
2013	0.98 ± 0.00	1.00 ± 0.04
2014	0.97 ± 0.00	0.77 ± 0.03
2015	0.96 ± 0.00	0.71 ± 0.03
2016	0.98 ± 0.00	0.69 ± 0.03
Montane		
2013	1.01 ± 0.00	0.99 ± 0.03
2014	0.99 ± 0.00	1.01 ± 0.03
2015	1.00 ± 0.00	0.98 ± 0.03
2016	1.00 ± 0.00	0.90 ± 0.03

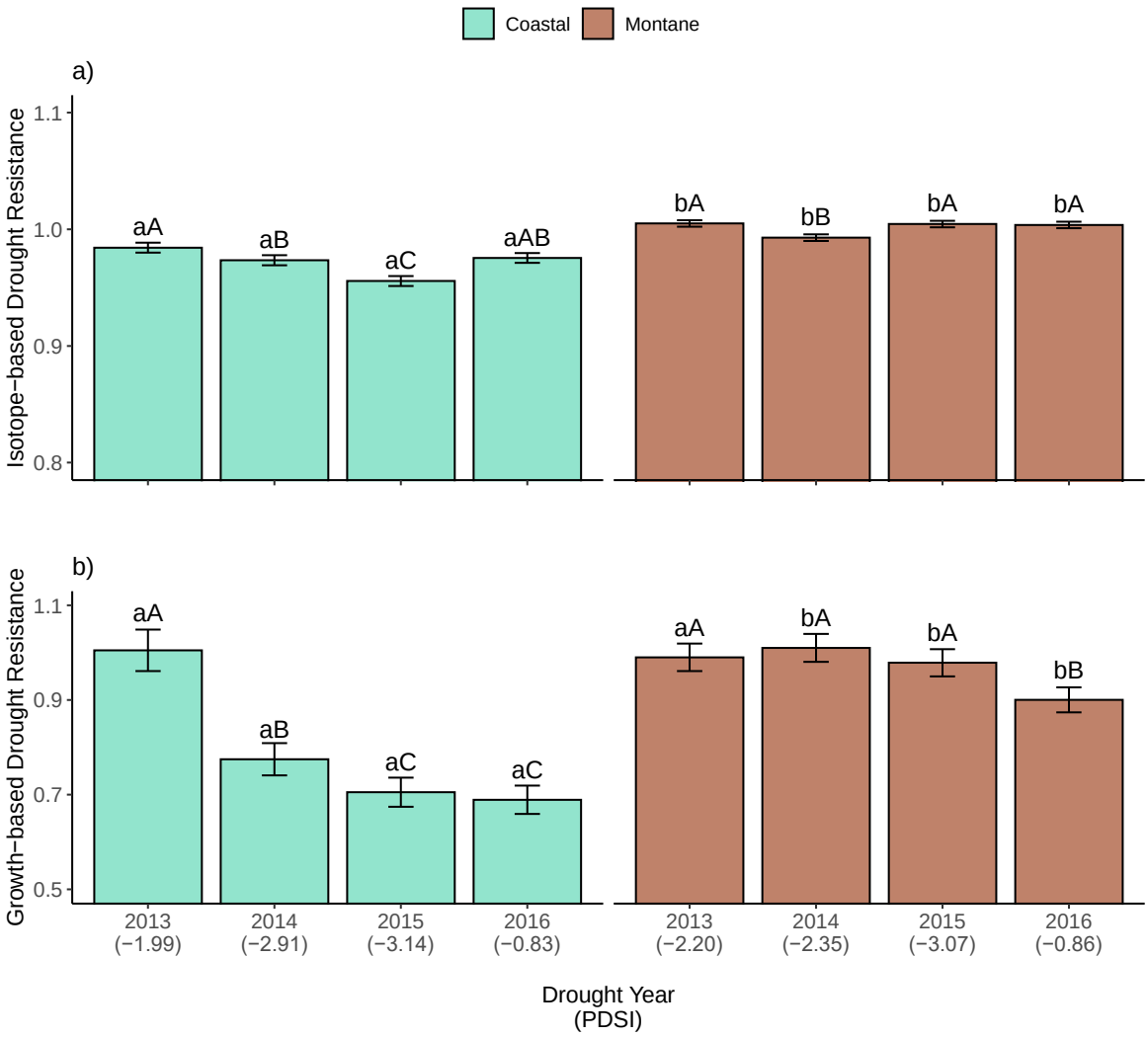

Figure 5. Mean (± SE) annual a) isotope-based and b) growth-based drought resistance by range type (*n* = 1010 tree-rings, 255 trees). Coastal species include Sitka spruce and western hemlock. Montane species include Shasta fir, Brewer spruce, sugar pine, and western white pine. Lowercase letters denote significant ($p < 0.05$) differences between the two range types within a year and uppercase letters denote differences among years within a range type. Mean annual Palmer Drought Severity Index (PDSI) for each range type is noted under each year. Note that the y-axis extends from 0.8 to 1.1 in plot a) and from 0.5 to 1.1 in plot b).

3.2 Drought Resistance in Wet and Dry Sites

For coastal trees (Sitka spruce and western hemlock), drought resistance varied across years and between wet and dry sites. Coastal trees at wet sites had significantly higher isotope-based drought resistance from 2013 to 2015 compared to coastal trees at dry sites (Table 5, Figure 6a). At both wet and dry sites, isotope-based drought resistance decreased steadily in coastal species between the first and third successive drought year. Notably, in 2016 when conditions became wetter, isotope-based drought resistance significantly recovered in coastal trees at dry sites but not at wet sites. Similar to isotope-based trends, growth-based drought resistance decreased steadily from 2013 to 2015 in both wet and dry coastal sites (Table 5, Figure 6b). However, unlike the high isotope-based resilience in 2016 for dry coastal sites, growth-based resilience was low at dry sites.

Table 5. Summary of mean (± SE) isotope- and growth-based drought resistance (DR) and 2016 resilience for coastal and montane trees at wet and dry sites.

Site	Isotope DR	Isotope Resilience	Growth DR	Growth Resilience
Coastal				
Wet	1.01 ± 0.01	0.99 ± 0.03	0.81 ± 0.09	0.61 ± 0.13
Dry	0.96 ± 0.01	0.98 ± 0.01	0.85 ± 0.08	0.79 ± 0.11
Montane				
Wet	1.00 ± 0.00	0.99 ± 0.00	1.00 ± 0.05	0.98 ± 0.09
Dry	1.00 ± 0.00	1.02 ± 0.01	0.97 ± 0.04	0.82 ± 0.04

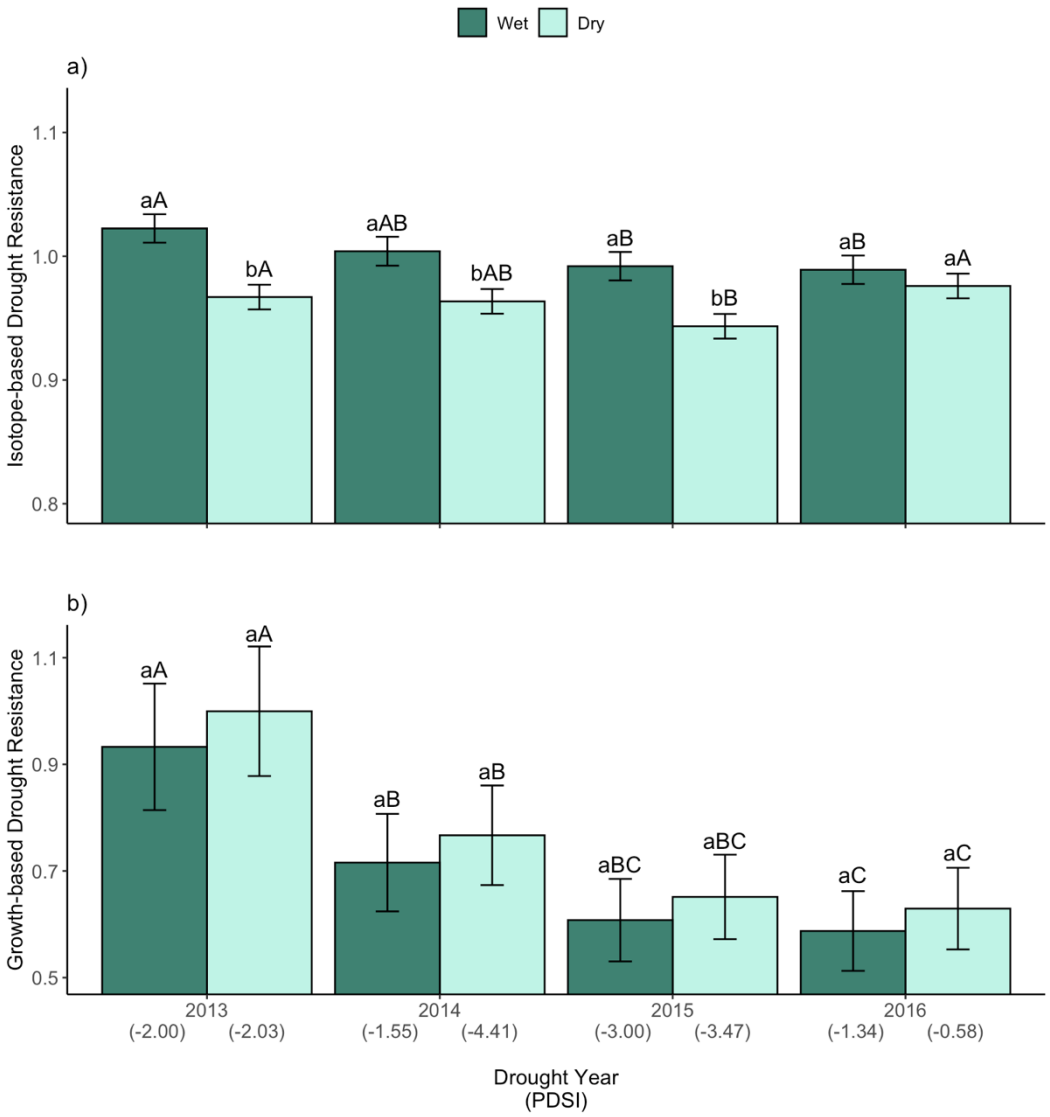

Figure 6. Mean (± SE) annual a) isotope-based and b) growth-based drought resistance for trees at the two wettest and driest coastal sites for Sitka spruce and western hemlock (n = 139 tree-rings, 35 trees). Lowercase letters denote significant ($p < 0.05$) differences between wet and dry habitats within a year and uppercase letters denote differences among years within a habitat type (wet or dry). Mean annual Palmer Drought Severity Index (PDSI) for each habitat type is noted under each year. Note that the y-axis extends from 0.8 to 1.1 in plot a) and from 0.5 to 1.1 in plot b).

For montane trees (Shasta fir, Brewer spruce, sugar pine, and western white pine), isotope- and growth-based drought resistance varied across years and between wet and dry sites. At wet sites, montane trees exhibited no significant differences in isotope-based drought resistance among years during or after the drought (Table 5, Figure 7a). While isotope-based drought resistance was similar between montane trees at wet and dry sites in 2013 and 2014, it significantly increased at dry sites in 2015 and 2016. Growth response at wet sites mirrored the stability detected in isotope-based measurements and did not significantly vary among successive drought years (Table 5, Figure 7b). In contrast, growth-based drought resistance at dry montane sites showed no significant change during the drought but then significantly declined in 2016.

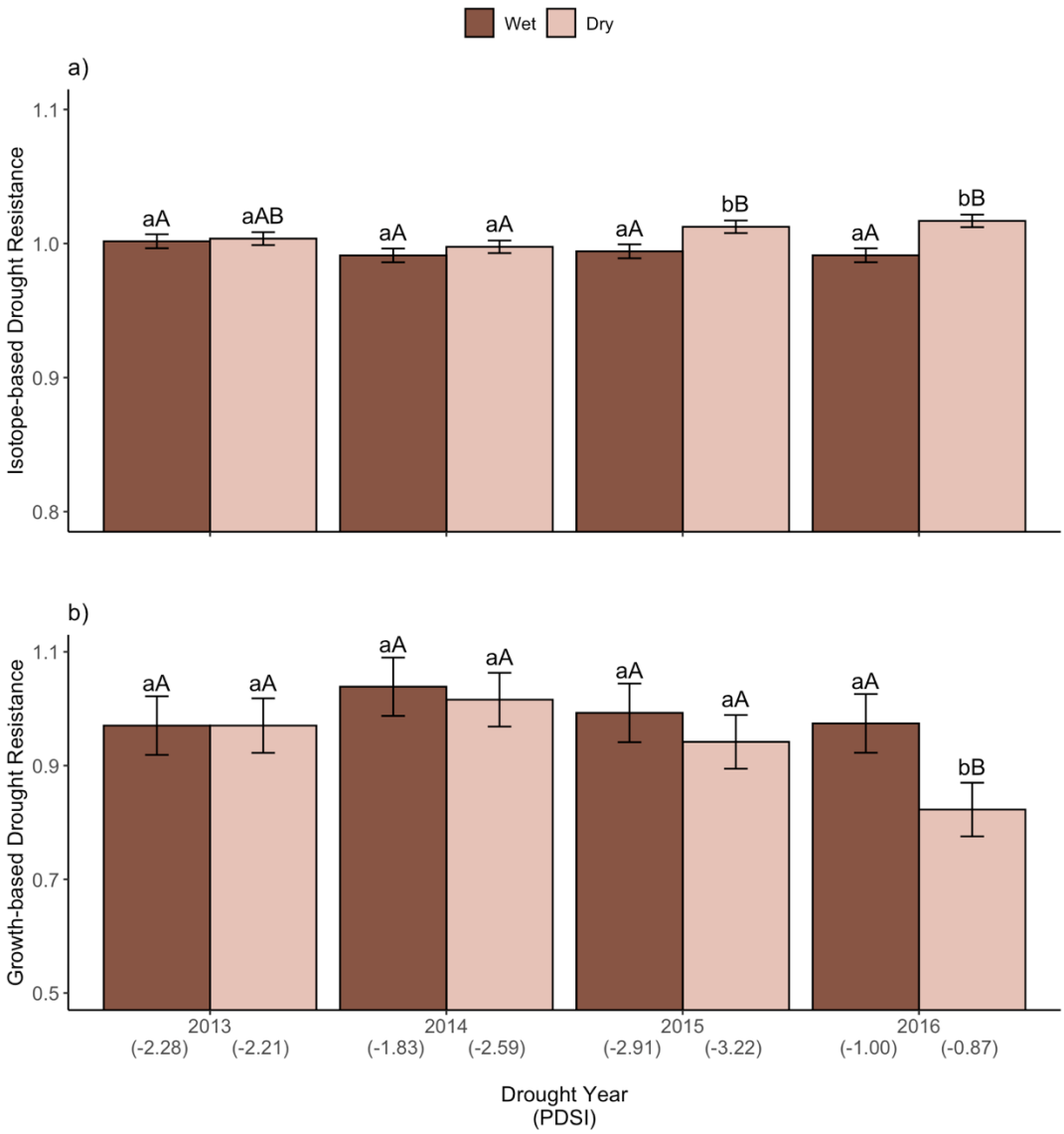

Figure 7. Mean (± SE) annual a) isotope-based and b) growth-based drought resistance for trees at the two wettest and driest montane sites for each species (*n* = 294 tree-rings, 75 trees). Montane species include Shasta fir, Brewer spruce, sugar pine, and western white pine. For Shasta fir, only one wet site was included in this analysis. Mean Palmer Drought Severity Index (PDSI) for each precipitation category is noted under each year. Lowercase letters denote differences in drought resistance between wet and dry sites within a year, while uppercase letters denote differences in drought resistance among years within a habitat type. Note that the y-axis extends from 0.80 to 1.10 in plot a) and from 0.50 to 1.10 in plot b).

3.3 Effects of Competition, Climate, Site and Tree Characteristics on Species-level Tree Physiology

Across all six conifer species, Sitka spruce, western hemlock, and Brewer spruce had the greatest (positive) $\Delta^{13}C$ response to drier moisture conditions as measured by PPT_{wy} (Figure 8a). Notably, PPT_{wy} varied more spatially than temporally throughout the Brewer spruce sites, while it varied both spatially and temporally throughout Sitka spruce and western hemlock sites (Figure 8). These three species either are at their southern range (Sitka spruce and western hemlock) or have a restricted range with local abundance (endemic Brewer spruce). In contrast, Shasta fir, sugar pine, and western white pine had relatively stable $\Delta^{13}C$ across both moisture conditions (sites) and years. The two coastal species also had higher $\Delta^{13}C$ than the four montane species throughout most of the study period.

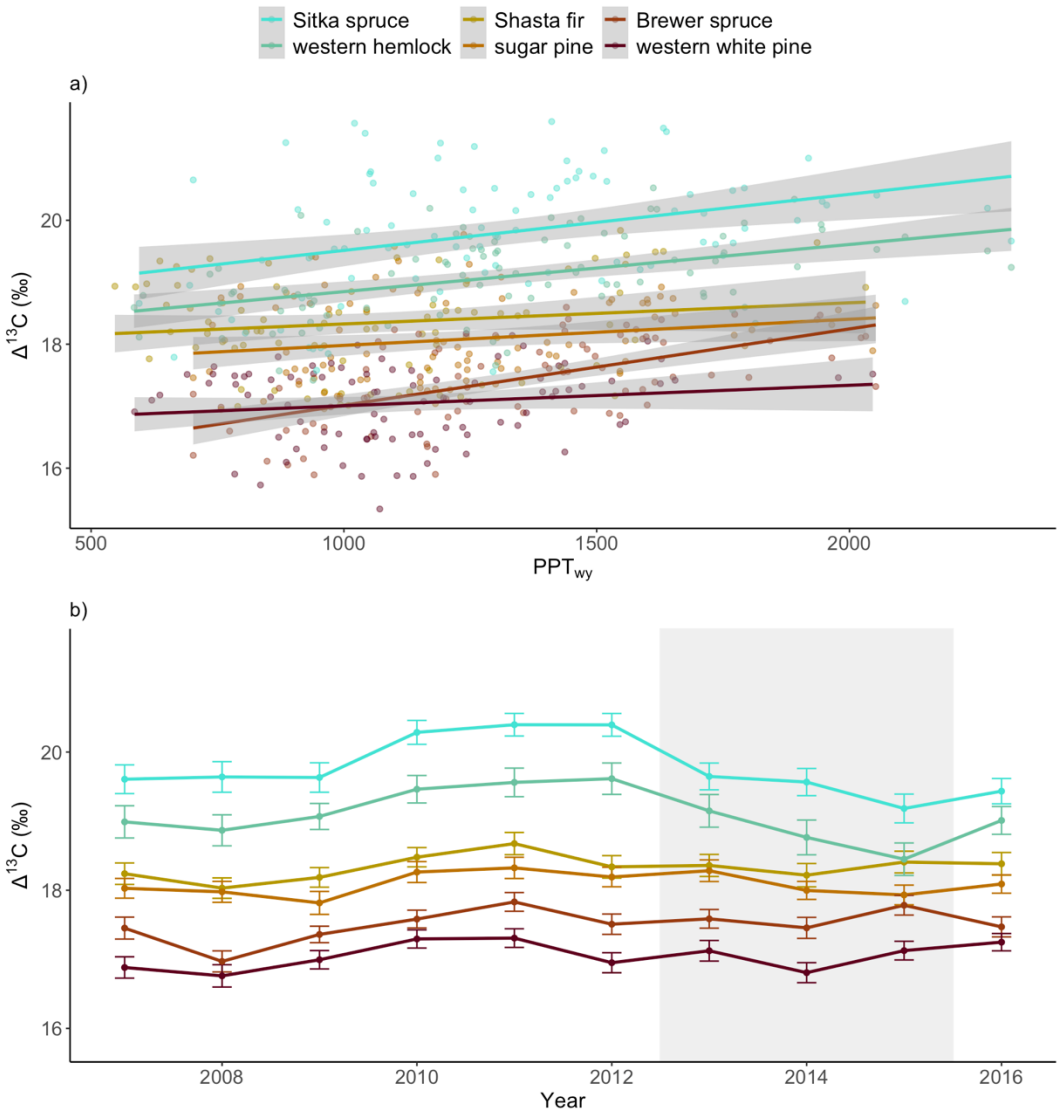

Figure 8. Mean annual ^{13}C discrimination ($\Delta^{13}C$) a) per species per site across a range of water-year precipitation (PPT_{wy}) values and b) per species throughout the study period. Grey area in a) denotes the 95% confidence interval for each regression line while in b) it highlights the drought years (2013 – 2015). Bars in b) represent standard error. Coastal species are shown in greens and montane species are shown in shades of brown.

Coastal Species: Sitka spruce and western hemlock

Physiological response was positively correlated with PPT_{wy} in both coastal species, as well as in the pooled coastal model (Figure 9). The best mixed-effects model for Sitka spruce (*n* = 440 tree-rings with 44 trees) included an interaction between PPT_{wy} and HLI, with trees at sites with higher HLI experiencing lower $\Delta^{13}C$ with lower PPT_{wy} (Table 6, Figure 9a, Appendix D Figure D1). The best model for western hemlock (*n* = 307 tree-rings with 31 trees) included PPT_{wy} and TPH (Table 6, Figure 9b). Water-year precipitation had a positive effect on $\Delta^{13}C$, while TPH had a negative effect on $\Delta^{13}C$. The best model for pooled coastal species (*n* = 747 tree-rings with 75 trees) included an interaction between PPT_{wy} and TPH, with trees with high TPH having lower $\Delta^{13}C$ with lower PPT_{wy} than those with lower TPH (Table 6, Figure 9c, Appendix D Figure D2).

Table 6. Top linear mixed-effects models for the two coastal species and for pooled coastal species. Predictor variables include: water-year precipitation (PPT_{wy}), heat load index (HLI), and trees per hectare (TPH). The best model is bolded.

Model	Predictors	df	logLik	AICc	ΔlogLik	ΔAICc
Sitka spruce	**PPT_{wy}*HLI**	9	-511.7	1041.8	0.0	0.0
	PPT_{wy}, HLI	8	-514.9	1046.0	3.2	4.2
	PPT_{wy}	7	-518.4	1051.1	6.7	9.3
	HLI	7	-521.3	1056.8	9.6	15.0
Western hemlock	PPT_{wy}*TPH	8	-353.2	722.9	0.0	0.0
	PPT_{wy}, TPH	7	-355.1	724.5	1.9	1.6
	PPT_{wy}	6	-357.4	727.0	4.2	4.1
	TPH	6	-360.9	734.0	7.7	11.1
Pooled	**PPT_{wy}*TPH**	9	-874.6	1767.5	0.0	0.0
	PPT_{wy}, TPH	8	-878.7	1773.6	4.1	6.1
	PPT_{wy}	7	-881.4	1777.0	6.8	9.4
	TPH	7	-891.3	1796.7	16.6	29.1

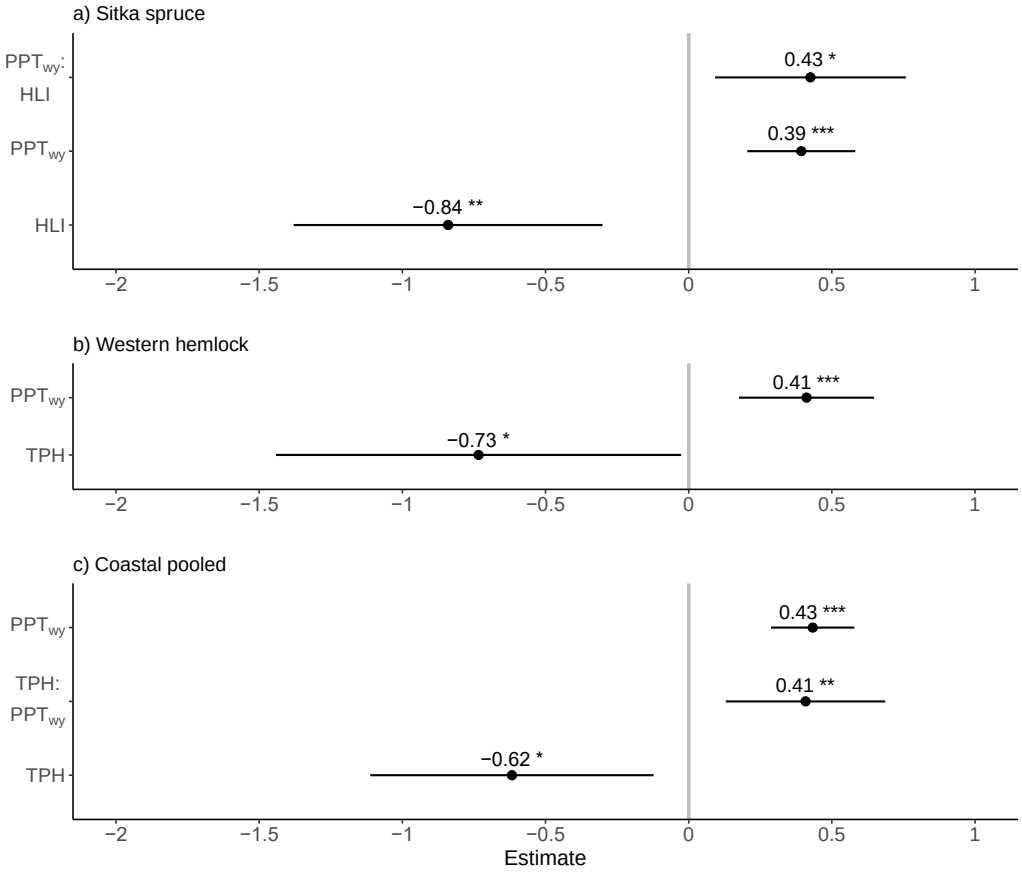

Figure 9. Model estimates with 95% confidence intervals of each predictor variable in the best models for explaining variation in ^{13}C discrimination ($\Delta^{13}C$, years 2007 – 2016) in a) Sitka spruce (n = 440 tree-rings with 44 trees), b) western hemlock (n = 307 tree-rings with 31 trees), and c) the coastal species pooled (Sitka spruce and western hemlock, n = 747 tree-rings with 75 trees). Predictor variables include: water-year precipitation (PPT_{wy}), heat load index (HLI), and trees per hectare (TPH). Asterisks denote significance levels of p-values (* < 0.05, ** < 0.01, and *** < 0.001).

Montane Species: Shasta fir, Brewer spruce, sugar pine, and western white pine

The best models for physiological response in montane species had varied predictors, making pooled analysis of all montane species inappropriate (but see Table 7 and Appendix E). The best model for $\Delta^{13}C$ in Shasta fir (n = 448 tree-rings with 45 trees)

included a significant interaction between PPT_{wy} and DBH (Table 7, Figure 10a, Appendix D Figure D3). This interaction showed that all trees had similar $\Delta^{13}C$ during high water-year precipitation, but that large DBH trees had lower $\Delta^{13}C$ during low PPT_{wy} compared to smaller DBH trees.

The best model for $\Delta^{13}C$ in Brewer spruce (n = 442 tree-rings with 45 trees) included total Hegyi index and an interaction between PPT_{wy} and T_{min} (Table 7, Figure 10b, Appendix D Figure D4). Total live tree Hegyi index had a positive effect on $\Delta^{13}C$. While T_{min} had little effect on $\Delta^{13}C$ when PPT_{wy} was high, low T_{min} was correlated with steeper declines in $\Delta^{13}C$ under lower values of water-year precipitation.

The two pine species had simpler models. The best model for $\Delta^{13}C$ in sugar pine (n = 438 tree-rings with 45 trees) included elevation and PPT_{wy} (Table 7, Figure 10c). Water-year precipitation was positively correlated with $\Delta^{13}C$, while elevation was negatively correlated with sugar pine $\Delta^{13}C$. The best model for $\Delta^{13}C$ in western white pine (n = 448 tree-rings with 45 trees) included PPT_{wy}, 30-year average precipitation, and TPH (Table 7, Figure 10d). Both precipitation terms had a significantly positive correlation with western white pine $\Delta^{13}C$, while TPH had a negative correlation on western white pine $\Delta^{13}C$.

Table 7. Top linear mixed-effects models for the four montane species and for pooled montane species. Predictor variables include: water-year precipitation (PPT_{wy}), diameter at breast height (DBH), maximum annual temperature (T_{max}), total live tree Hegyi index (CI_l), minimum annual temperature (T_{min}), elevation (Elev), serpentine soil (Serp), 30-year average precipitation (PPT_{30}), trees per hectare (TPH), and species (SP). Best models are bolded.

Model	Predictors	df	logLik	AICc	ΔlogLik	ΔAICc
Shasta fir	**PPT_{wy}*DBH, T_{max}**	9	-284.8	588.0	0.0	0.0
	PPT_{wy}*DBH	8	-287.7	591.8	2.9	3.8
	PPT_{wy}, DBH, T_{max}	8	-288.3	593.0	3.5	5.0
	PPT_{wy}, T_{max}	7	-291.4	597.1	6.6	9.2
	PPT_{wy}, DBH	7	-292.0	598.3	7.2	10.4
Brewer spruce	**PPT_{wy}*T_{min}, CI**	10	-340.7	702.0	0.0	0.0
	PPT_{wy}*T_{min}	9	-344.6	707.6	3.9	5.6
	PPT_{wy}, T_{min}, CI	9	-344.6	707.6	3.9	5.6
	PPT_{wy}, T_{min}	8	-348.2	712.8	7.5	10.8
Sugar pine	PPT_{wy}, Elev, Serp	7	-387.1	788.4	0.0	0.0
	PPT_{wy}, Elev	6	-388.3	788.9	1.3	0.5
	PPT_{wy}, Serp	6	-388.5	789.3	1.5	0.9
	PPT_{wy}	5	-391.4	792.9	4.3	4.4
	Serp	5	-397.7	805.5	10.6	17.1
Western white pine	**PPT_{wy}, TPH, PPT_{30}**	8	-343.9	704.0	0.0	0.0
	PPT_{wy}, TPH	7	-348.5	711.2	4.6	7.1
	PPT_{wy}, PPT_{30}	7	-349.0	712.3	5.1	8.2
	PPT_{wy}	6	-351.5	715.1	7.6	11.1
Pooled	**PPT_{wy}*T_{min}, SP**	11	-1393.3	2808.7	0.0	0.0
	PPT_{wy}*T_{min}	8	-1403.2	2822.4	9.9	13.7
	PPT_{wy}, SP	9	-1408.9	2835.8	15.6	27.1

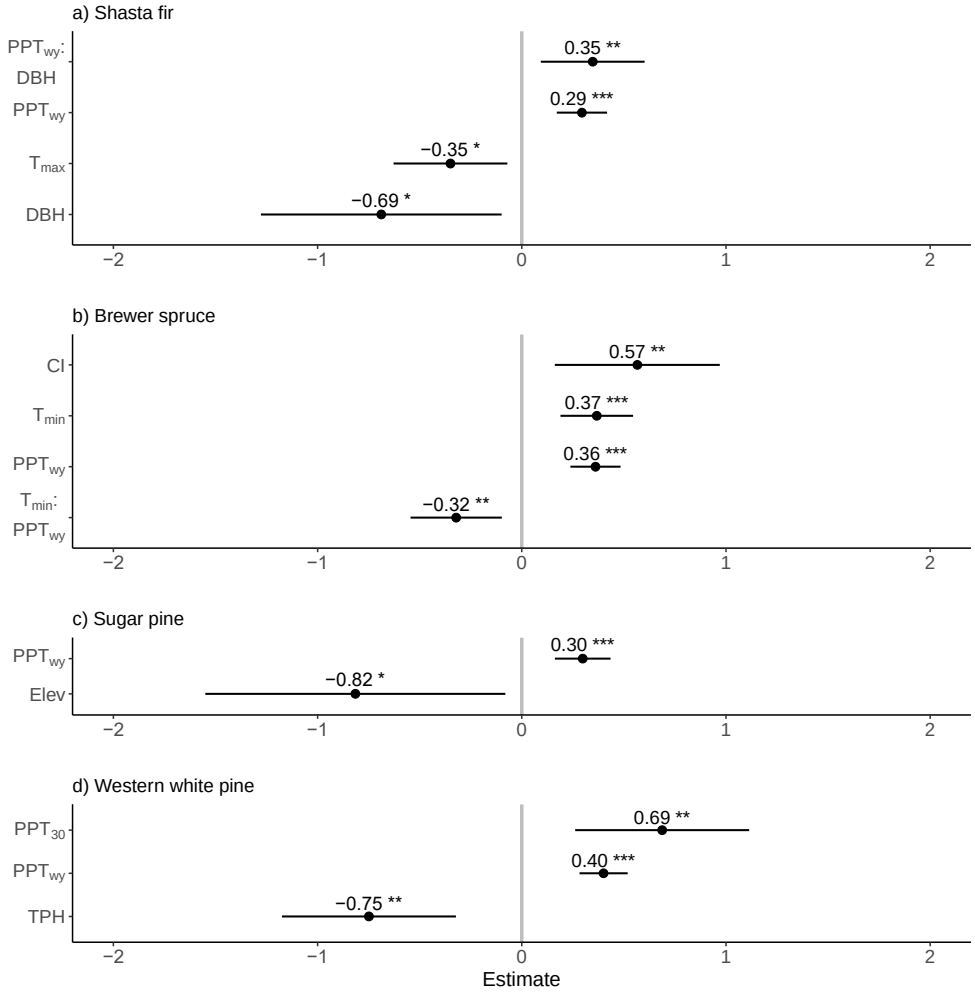

Figure 10. Model estimates with 95% confidence intervals of each predictor variable in the best models for explaining variation in ^{13}C discrimination ($\Delta^{13}C$, years 2007 – 2016) in a) Shasta fir (n = 448 tree-rings with 45), b) Brewer spruce (n = 442 tree-rings with 45 trees), c) sugar pine (n = 438 tree-rings with 45 trees), and d) western white pine (n = 448 tree-rings with 45 trees). Predictor variables include: water-year precipitation (PPT_{wy}), diameter at breast height (DBH), maximum annual temperature (T_{max}), total live tree Hegyi index (CI), minimum annual temperature (T_{min}), elevation (Elev), 30-year average precipitation (PPT_{30}), and trees per hectare (TPH). Asterisks denote significance levels of p-values (* < 0.05, ** < 0.01, and *** < 0.001).

4. DISCUSSION

The two coastal species (Sitka spruce and western hemlock) were more sensitive to drought than the four montane species (Shasta fir, Brewer spruce, sugar pine, and western white pine). Moisture conditions (wet or dry) affected coastal trees' response to drought such that coastal trees at dry sites had more immediate reactions to drought, especially with regard to physiological ($\Delta^{13}C$) response, compared to coastal trees at wet sites. Water-year precipitation and TPH were significantly related to coastal trees' physiological response, and likely contributed to the differences in resistance and resilience in wet and dry coastal sites. In contrast, montane species maintained high resistance and resilience values across moisture conditions, with environmental factors contributing to each species' physiological response in different ways. Of particular note were the varied effects of competition and temperature on annual $\Delta^{13}C$ values among the four montane species. These results illustrate the importance of site and climate conditions affecting conifer responses differently throughout the montane region. Thus, conifers in northern California would benefit from site-specific management.

4.1 Drought Resistance in Coastal and Montane Conifer Species in Northern California

Two overall trends distinguished the coastal species (Sitka spruce and western hemlock) from the montane species (Shasta fir, Brewer spruce, sugar pine, and western

white pine). Both coastal species maintained higher $\Delta^{13}C$ and exhibited a larger range of $\Delta^{13}C$ throughout the study period compared to the four montane species (Figure 8). Coastal species also experienced a decline in isotope-based drought resistance throughout the drought, while montane species remained relatively stable (Figure 5).

This difference in drought resistance between coastal and montane species may indicate a difference in drought survival strategies between these two range types, with coastal species varying stomatal conductance depending on drought conditions and montane species maintaining relatively even stomatal conductance regardless of drought conditions. Previous work indicates that western hemlock exercises relatively high stomatal regulation during water stress (Bond & Kavanagh, 1999) and that Sitka spruce xylem has a relatively high vulnerability to cavitation (Jackson et al., 1995). These characteristics suggest that increased stomatal regulation during severe drought may be necessary to prevent hydraulic damage in both of these coastal species, especially since stomatal regulation is positively correlated to vulnerability to cavitation in trees and shrubs elsewhere in the western United States (Baker et al., 2019; Pivovaroff et al., 2018).

In contrast, the consistent level of isotope-based drought resistance in montane species suggests that these conifers do not notably increase stomatal regulation during water stress, or at least not until they experience more water stress than they did during the study period at these sites in northern California. Although low stomatal regulation is

a survival strategy for many plants with inconsistent or limited access to water (Klein, 2014; Pivovaroff et al., 2018), this lack of plasticity may become problematic for the two pine species, since many pine species are known to be relatively vulnerable to hydraulic failure compared to other genera in Pinaceae (Martínez-Vilalta et al., 2004). The combination of limited stomatal regulation and high vulnerability to xylem cavitation could result in lower resilience post-drought in the driest areas of sugar and western white pine ranges due to runaway embolism and loss of hydraulic capacity (Adams et al., 2017; Baker et al., 2019). This could explain the noticeably low growth-based resilience measured in western white pine in 2016 (Appendix B).

Despite different physiological drought response strategies, both coastal and montane species experienced a lag in growth-based resilience in 2016 without a commensurate delay in isotope-based resilience (Figure 5). One possible explanation for this difference between isotope- and growth-based metrics is that in 2016 when conditions became wetter, both coastal and montane trees allocated more photosynthate to replenishing non-structural carbohydrate (NSC) stores depleted during the drought. This carbon sink would likely be a high priority after prolonged drought (Oberhuber et al., 2011), as NSCs are important for osmoregulation and are thought to play a role in reversing embolism (Nardini et al., 2011; Sala et al., 2012) and subsequently preventing drought-related mortality (Adams et al., 2017; Dickman et al., 2015; Kannenberg et al., 2018; Martínez-Vilalta et al., 2016). The fact that NSC depletion occurs in conifers

across a range of stomatal regulation strategies (Dickman et al., 2015) could explain the difference between isotope- and growth-based 2016 resilience measured in both coastal and montane species. Another possible explanation for the 2016 difference between increased $\Delta^{13}C$ and decreased growth is that trees allocated newly available photosynthate towards fine root production to improve water uptake after experiencing three years of drought (Doughty et al., 2014; Magnani et al., 2002; Meier & Leuschner, 2008).

4.2 Drought Resistance in Wet and Dry Sites

Coastal Species: Sitka spruce and western hemlock

Trees at dry coastal sites experienced more immediate changes in isotope-based drought resistance and resilience (2016) than trees at wet sites, while growth-based drought resistance and resilience were similar for trees across wet and dry sites (Table 5, Figure 6). The greater immediate sensitivity to drought corroborates past evidence that the stomata of trees from dry areas are more responsive to drought than conspecifics from wet areas (Isaac-Renton et al., 2018). This suggests that coastal species, even at the southern edge of their range where they are potentially more water-stressed, are still capable of maintaining physiological plasticity. In this case, it is also important to note that both moisture conditions and stand structure likely affected these trees' drought

response. Wet sites had a 30-year annual precipitation average of 1818 mm and were dominated by fewer, larger, overstory trees such as coast redwood (*Sequoia sempervirens*. (Don) Endl.), Sitka spruce, and western hemlock (Figure 11a). Meanwhile, dry sites had a 30-year annual precipitation average of 1095 mm and were composed of more densely packed, heterogenous woody plant communities, including a variety of tall (tree form) shrubs and small tree species of cascara (*Frangula purshiana* (DC) JG Cooper), Pacific rhododendron (*Rhododendron macrophyllum* Don), and Pacific wax-myrtle (*Myrica californica* Cham., Figure 11b). The difference in average precipitation and plant community (and therefore canopy composition, Figure 11, Appendix F) suggests that wet sites were more light-limited, while dry sites were more water-limited. Across the northern hemisphere, plant species often are either shade-tolerant (i.e., adapted to light-limited environments) or drought-tolerant (i.e., adapted to water-limited environments; Niinemets & Valladares, 2006; Rueda et al., 2017). The site-level precipitation and stand structure information combined with the variable drought response of the same two coastal species in wet and dry sites presented here could indicate that the trade-off between shade tolerance and drought tolerance among species also applies within species.

Figure 11. Site comparisons for coastal a) wet and b) dry habitats. Note the denser canopy and relatively fewer tree-sized (greater than five centimeters diameter at breast height) stems in a), and the more open canopy, denser shrub/small tree component, and greater number of tree-sized stems in b).

The lower stomatal regulation at wet sites and lack of notable rebound in $\Delta^{13}C$ may mean that coastal species were less responsive to dry conditions from 2013 – 2015 than trees adapted to dry sites. Given that temperatures are projected to rise 2.8 to 5 °C in northwestern California during the next century (Grantham, 2018), it is possible that coastal species in wet areas may begin to experience declines in hydraulic capacity (and subsequently, growth) caused by insufficient stomatal regulation. However, wet coastal sites also experienced relatively drier conditions than dry sites in 2016 (PDSI values of -1.34 and -0.58, respectively, Table 5, Figure 6), so it is also possible that the differences in resilience measured here have more to do with local drought conditions than with adaptation to historic site conditions. Due to the short post-drought measurement period (2016) and the difference in PDSI values between wet and dry sites, more definitive

research is needed to understand the true implications of the differences in isotope-based resilience measured here.

The stomatal sensitivity of trees from dry sites may indicate that Sitka spruce and western hemlock at the southern edge of their range are well-adapted to dealing with multi-year dry conditions. Although high stomatal regulation during drought has generally resulted in higher mortality due to carbon starvation in more arid environments (McDowell et al., 2010; Trifilò et al., 2017), these results suggest that high stomatal regulation may be a successful strategy for coastal species under warmer conditions and prolonged drought. Coastal trees at dry sites also had marginally higher growth-based drought resistance and resilience than coastal trees at wet sites (Table 5, Figure 6), which could mean that trees at dry sites had more carbon stores to draw on for maintenance and repair during times of reduced stomatal conductance.

Montane Species: Shasta fir, Brewer spruce, sugar pine, and western white pine

Trees in both wet and dry montane sites exhibited little variation in isotope-based drought resistance during the drought, but trees at dry sites experienced a small but significant increase in 2015 and 2016 (Table 5, Figure 7). This increase in isotope-based drought resistance and resilience at montane dry sites was coupled with declines in growth-based drought resistance, which suggests that the change in $\Delta^{13}C$ may have resulted from reduced photosynthesis due to loss of hydraulic capacity from cavitation

instead of from an increase in stomatal conductance (Hubbard et al., 2001; Peguero-Pina et al., 2018). Since montane trees at wet sites had relatively consistent isotope- and growth-based drought resistance throughout the drought, it seems especially likely that the trend detected in montane dry sites was caused by a decrease in hydraulic capacity that resulted from unregulated stomatal conductance paired with high evapotranspirational demand.

Declines in hydraulic capacity are often linked to depletion of NSC stores, which could lead to slower embolism repair and explain the low growth-based resilience measured in 2016 at dry sites (Trifilò et al., 2017). Although the changes in both isotope- and growth-based drought resistance for montane trees at dry sites were small relative to the changes in isotope and growth-based metrics in some other studies (Barber et al., 2000; Bottero et al., 2017; McDowell et al., 2003), the lag in growth-based resilience in trees at dry sites in 2016 may be cause for concern if trees are not able to sufficiently replenish their NSC stores before the next major drought. However, since this study only included one post-drought year, more research is needed to determine how long it would take trees at dry sites to recover to pre-drought levels.

Montane trees at wet sites did not experience any significant changes in isotope- or growth-based metrics throughout the entire drought and post-drought period. This suggests that these trees had adequate resources to survive the drought, and may not be at immediate risk for drought-induced mortality. The relatively high overall drought

resistance may be attributable to these trees living in relatively mild habitats in central parts of their range.

4.3 Effects of Competition, Climate, and Site and Tree Characteristics on Species-level Tree Physiology

Coastal Species: Sitka spruce and western hemlock

All three coastal models (Sitka spruce, western hemlock, and pooled) included water-year precipitation, which had a consistently positive correlation with $\Delta^{13}C$ (Table 6, Figure 9). In the pooled model, trees with higher TPH experienced lower $\Delta^{13}C$ in dry conditions, but similar $\Delta^{13}C$ during wet conditions (Appendix D Figure D2). Although the interaction between TPH and PPT_{wy} was technically not significant for the western hemlock model ($p = 0.054$), western hemlock also displayed reductions in $\Delta^{13}C$ during dry water-years with higher TPH. These trends may be a result of differences in microclimate between wet and dry sites. Specifically, many coastal trees at dry sites grew in areas with large shrubs and understory tree species (i.e., stands characterized by smaller trees and more TPH on average), while many coastal trees at wet sites primarily grew near other overstory trees (i.e., stands characterized by larger trees and fewer TPH on average, Figure 11). While the community composition at dry sites likely resulted in greater canopy openness (i.e., greater light), this forest structure also may have fostered

higher evapotranspirational demand, especially during the drought (Caldeira et al., 2015). In contrast, the community composition at wet sites likely resulted in more closed canopies (i.e., less light) and dampened evapotranspirational demand (Ringgaard et al., 2012). The difference in light access was likely also affected by the frequency of fog cover along the coast, which generally was greater at wet (and relatively northern) sites compared to dry sites (Torregrosa et al., 2016). Greater access to light at dry sites may have resulted in greater stomatal conductance, but also greater photosynthetic capacity when water was not limited, explaining the similar $\Delta^{13}C$ during wet conditions. The greater evapotranspirational demand during drought may have resulted in lower stomatal conductance, and the subsequently lower $\Delta^{13}C$ during dry conditions. Additionally, trees at wet sites may have experienced marginally lower pre-drought stomatal conductance due to a combination of more fog as well as light competition in a denser overstory, but less change in stomatal conductance during drought due to less evapotranspirational demand. This interaction between moisture conditions and plant community composition may therefore be partially responsible for the lower isotope-based drought resistance measured in coastal trees at dry sites, which started with slightly higher baseline $\Delta^{13}C$ pre-drought and experienced lower $\Delta^{13}C$ during the drought (Figure 6 and Appendix G). In Sitka spruce, $\Delta^{13}C$ was lower at sites with greater HLI during dry water-years, but was similar across all sites when PPT_{wy} was higher. Additionally, HLI was negatively

correlated with 30-year precipitation in Sitka spruce, which suggests that similar light and water dynamics may influence Sitka spruce $\Delta^{13}C$.

Species was not an important factor in predicting $\Delta^{13}C$ in the coastal pooled model, suggesting that at least in the southern part of their ranges, Sitka spruce and western hemlock exhibit similar responses to drought (Table 6, Figure 9). Thus, estimating future tree response to moisture variability could probably be cautiously applied to multiple coastal species. This may be a helpful tactic in areas where one or both of these species are sparse and sampling a large number of either is prohibitively expensive.

Montane Species: Shasta fir, Brewer spruce, sugar pine, and western white pine

All four montane species had similar drought resistance, but the factors contributing to each species' drought response differed. Water-year precipitation was consistently positively correlated with $\Delta^{13}C$, but the significance of competition and site characteristics on $\Delta^{13}C$ varied across the four species (Table 7, Figure 10). Competition's variable effect on isotope-based drought sensitivity in this study is in line with other studies in the United States and Switzerland that have reported nuanced competition effects on growth (Carnwath & Nelson, 2016; Gillerot et al., 2021).

Competition had no effect or a positive effect on $\Delta^{13}C$ in Shasta fir and Brewer spruce, respectively. These two species also had the two highest average competition

indices (Table 1). However, the lack of a significant competition effect in Shasta fir $\Delta^{13}C$ in this study should not be taken as evidence that drought response in Shasta fir is completely unaffected by competition. Intraspecific competition can significantly affect Shasta fir mortality in conjunction with high pathogen loads by enhancing drought stress and likelihood of transmission of certain pathogens (DeSiervo et al., 2018). Unhealthy trees were excluded from this study, leaving open the possibility that there may be a meaningful interaction among competition, vulnerability to pathogens, and drought resistance that was not evident in the live trees sampled in this study. Diameter was a significant factor for this species, corroborating past findings that tree size can have a negative impact on drought response (Bohner & Diez, 2021; Gillerot et al., 2021). Large trees are more vulnerable to drought due to the hydraulic stress associated with great height, higher evaporative demand associated with large crowns, longer xylem repair time, and greater attractiveness to parasites (Bennett et al., 2015; Trugman et al., 2018). All of these mechanisms could put large Shasta firs at greater risk of mortality in the future, especially in stands with additional pre-existing stressors or if more frequent droughts become common. However, some studies have found that large trees of various species are less vulnerable to drought due to deeper roots and more tolerance to low water potentials (Dawson, 1996; Duursma et al., 2011; Goulden & Bales, 2019; Grote et al., 2016). Large trees growing in areas with access to deeper water sources may be less vulnerable to additional drought stress compared to large trees with less water access.

It is possible that the positive correlation of competition with $\Delta^{13}C$ in Brewer spruce actually results from a shade-induced decrease in photosynthesis rather than increased stomatal conductance (Linares et al., 2009). Given that both 30-year average precipitation and annual precipitation rates at Brewer spruce sites are higher than those of other montane species, light limitation seems especially likely (Appendix A Table A2). Alternatively, the higher $\Delta^{13}C$ values in Brewer spruce in competitive stands could reflect baseline stomatal conductance rather than light-limited reductions in photosynthesis. Relatively lower $\Delta^{13}C$ in less competitive stands could reflect a decrease in stomatal conductance due to more open canopy conditions with increased evapotranspirational demand. The latter scenario would corroborate other studies that have shown spruce species to be adapted to low light situations, and in some cases more vulnerable to decreased stomatal conductance in high light intensity (Riikonen et al., 2016; Urban et al., 2012; Waring et al., 1975). Because Brewer spruce does not generally compete well in high-density stands (Waring et al., 1975), it may persist in these conditions via high stomatal conductance despite vigorous competition for light in the mid to upper canopy. In addition, $\Delta^{13}C$ in Brewer spruce decreased less in dry conditions when minimum annual temperature was high. Notably, the three highest minimum temperatures in the Brewer spruce dataset were above freezing, and were all greater than a half standard deviation away from the mean minimum temperature. Temperatures above freezing lead to a greater capacity for trees to utilize water earlier in the growing season (Hultine &

Marshall, 2000). This may have allowed Brewer spruce to take advantage of any available water early in the growing season during dry years, and consequently maintain higher $\Delta^{13}C$ than possible during comparable dry conditions when T_{min} was cooler and early water pools were not available.

Competition had a negative or no effect on $\Delta^{13}C$ in western white pine and sugar pine, respectively. Given the small scope of this study (9 sites per species) relative to the range of western white pine and sugar pine, it is possible that climate, site characteristics, and/or competition may interact across a broader geographic region. Specifically, both western white pine and sugar pine can both occupy much drier sites elsewhere in their ranges, where competitive stand conditions may be more stressful, so sampling across a broader range may elucidate more nuanced findings on possible interactions between competition and average annual precipitation. Elevation had a negative correlation with sugar pine $\Delta^{13}C$, which could be a result of the significant negative correlation of minimum annual temperature with elevation (Appendix H Figure H1). Stomatal conductance decreases in response to decreased temperature (Urban et al., 2017), and other studies on western conifers have found similar decreases in $\Delta^{13}C$ with elevation, especially in pine species (Hultine & Marshall, 2000; Schwarz et al., 1997). Although the cause of these trends is debated, one plausible explanation is that stomatal conductance is negatively correlated with soil temperature (Hultine & Marshall, 2000), which is generally correlated with air temperature. Higher minimum soil temperatures at low

elevation sites may allow trees to begin photosynthesizing earlier and take advantage of early season moisture availability. This would imply greater stomatal conductance during earlywood production and higher mean $\Delta^{13}C$ per ring. Another possible explanation for the negative correlation of sugar pine $\Delta^{13}C$ is that the diffusion rate of CO_2 into needles may decrease with elevation due to the slower movement of molecules at low temperatures. This may be especially true for pines since stomatal density in this genus has been found to decrease with elevation, although mid-elevation stomatal density may increase depending on the species (Schoettle & Rochelle, 2000; Zhou et al., 2012).

4.4 Management Implications and Future Directions

Drought survival strategies differed between coastal and montane species in this study, and may indicate likely causes of mortality if droughts become longer, more severe or both in the future. Using the framework outlined in Gessler et al. (2018), the conservative stomatal regulation strategy employed by coastal species may predispose these trees to death by carbon starvation if droughts become longer, while the less regulated strategy employed by montane species may cause death by hydraulic failure, especially if droughts increase in severity or frequency. However, these strategies are augmented by site conditions, especially in coastal species. The lack of swift stomatal response in coastal species at wet sites may be a precursor to high mortality in certain

parts of the southern end of the two coastal species' ranges, which appear to be shifting northward (Monleon & Lintz, 2015). However, the responsiveness of coastal species at dry sites might indicate that well-established trees in these dry southern sites may persist depending on the length of droughts in the future, even if younger conspecifics do not.

Various thinning treatments have been explored for improving stand structure and heterogeneity in coastal redwood forests in this region (O'Hara et al., 2012; Soland et al., 2021; Teraoka & Keyes, 2011), and this study suggests that thinning may also be a successful strategy for improving drought response in Sitka spruce and western hemlock stands. In both western hemlock and the pooled model, greater stand density was correlated with lower $\Delta^{13}C$ during dry years, with no obvious physiological benefit during wet years. Thinning dense, coastal sites farther north would likely increase light availability and photosynthetic capacity, which could result in greater carbon stores to draw on during prolonged drought. Additionally, these trees would likely not be at greater risk of hydraulic failure from greater evapotranspirational demand brought on by a more open canopy since coastal species exerted relatively high stomatal regulation in response to drier conditions (Figure 5, Figure 8, Soland et al., 2021).

In drier areas near the southern edge of Sitka spruce and western hemlock ranges, exploring shrub-tree dynamics would be helpful. Although shrubs can have positive facilitative effects on sapling survival rates in stressful conditions (Redmond & Barger, 2013; Sthultz et al., 2007), there is little information on the effects of shrubs or

heterogenous canopy structures on the drought response of adult trees. Shrub encroachment has been linked with lower drought resistance and resilience in adult trees in the Mediterranean (Caldeira et al., 2015), while shrubs and trees have a mix of facilitative and competitive interactions elsewhere (Zou et al., 2005). Understanding how shrubs interact with Sitka spruce and western hemlock in the driest part of their range may be instrumental to predicting the extent of drought mortality and southern range constriction for these two coastal species.

Although montane species at dry sites appear to exercise minimal stomatal regulation during moisture limitation, it is less clear if they are at risk for range contraction. Further research would be helpful to more definitively track isotope- and growth-based recovery and resilience after prolonged and severe drought in both coastal and montane species, since recovery is a more reliable predictor of mortality than growth-based resistance in some conifer species (DeSoto et al., 2020). In addition, there is evidence that multiple water stressors (such as back-to-back droughts or severe drought following a water diversion event) can have a compounding effect on a tree's carbon budget (Schook et al., 2020). If extreme drought events begin to occur too frequently for trees to replenish NSC stores and allocate resources to damaged organs, conifers in northern California could end up at higher risk of mortality, especially in areas that have experienced lagged growth-based resilience.

Drought response in montane trees in this study was affected by different sets of factors, which may make prescriptive management solutions challenging. However, some recommendations can be made. Thinning treatments have proven effective at reducing drought stress in montane conifers in other studies in western North America (Bottero et al., 2017; Sohn et al., 2013; Vernon et al., 2018), and this study suggests that this strategy is likely appropriate in northern California, with a few additional considerations. Competition was negatively correlated with western white pine $\Delta^{13}C$ in this study. Additionally, this species does not seem to increase stomatal regulation during drought, but does exhibit some reductions in radial growth during post-drought recovery (Appendix B). If this reduction in growth is caused by hydraulic damage during the drought and subsequent reduced photosynthetic capacity, thinning treatments may increase moisture availability and help western white pine survive severe drought.

Competition was not significantly correlated with sugar pine or Shasta fir $\Delta^{13}C$, although other studies have found intraspecific competition to be negatively correlated tree vigor and/or radial growth in both of these species (DeSiervo et al., 2018; Slack et al., 2017). Both sugar pine and Shasta fir have the capacity to be dominant components in their respective environments, and are also prone to pathogens that may exacerbate competitive effects in dense stands of either species. In sugar pine and western white pine, white pine blister rust (*Cronartium ribicola* J. C. Fisch. Ex Raben) causes progressive branch death, which reduces photosynthetic capacity, and could make it more

difficult for these trees to replenish carbon stores post-drought. Although stand density may not increase the likelihood of blister rust infection (Campbell & Antos, 2000), trees in highly competitive stands may have less access to light, compounding the challenge of post-drought recovery, which could be problematic in the likely event of more frequent drought. Additionally, drought-stressed pines have less photosynthate available for resin production (Kane & Kolb, 2010, Slack et al., 2017), which may make these two pine species more vulnerable to bark beetle attack, particularly in crowded stands. Recent studies have noted an increase in Shasta fir mortality, especially in conjunction with high pathogen load (Bost, 2018; DeSiervo et al., 2018). Given the known interaction between pathogen load and intraspecific competition in relation to drought mortality in Shasta fir, it seems likely that thinning in high density stands would be helpful for mitigating future mortality, especially for large diameter trees. Therefore, although this study does not offer conclusive evidence on the effects of competition on healthy trees in this region for either species, thinning treatments should still be considered. However, more region-specific information is needed to explore the effects of competition, pathogen load, and drought on sugar pine physiology and drought resistance. Additionally, more baseline research on Shasta fir would be helpful in better understanding what stand structures would benefit most from thinning in this area.

Brewer spruce was the only species for which competition had a positive correlation with $\Delta^{13}C$, but the exact mechanisms underlying this trend remain ambiguous.

If $\Delta^{13}C$ is greater in highly competitive stands due to reduced photosynthetic capacity, moderate thinning treatments would likely be useful for reducing fuel load and increasing growth. Specifically, thinning in areas of high fire risk could prevent further mass mortality events for Brewer spruce, whose thin bark confers little fire protection (Thornburgh, 1990). However, Brewer spruce is not as tolerant to high evapotranspirational demand as other montane conifers (Waring et al., 1975) so thinning treatments should be approached with some caution. Although an analysis of BAI and total Hegyi index does suggest that the former scenario is plausible (Appendix H Figure H2), further research would be helpful to confirm this. Additionally, Brewer spruce lives in many disjunct and topographically variable pockets throughout the Klamaths, so site-specific studies are recommended when considering management strategies for this species.

Overall, despite range-specific drought responses and species-specific drivers of physiological status, all six of the species examined here had relatively high drought resistance and resilience to the 2012 – 2015 drought within the study area. These findings corroborate other studies that have found relatively low mortality to the 2012 – 2016 drought in northern California compared to southern California. This is likely due to the relatively shorter length and severity of the drought in the northern part of the state (Dong et al., 2019; Goulden & Bales, 2019) and biodiverse forest ecosystems less affected by bark beetle activity. However, these results provide important insights on potential

stressors on northern California forests that may be useful for preparing for novel drought scenarios in the face of growing climate-uncertainty.

LITERATURE CITED

Adams, H. D., & Kolb, T. E. (2004). Drought responses of conifers in ecotone forests of northern Arizona: Tree ring growth and leaf $\delta^{13}C$. *Oecologia*, *140*(2), 217–225. https://doi.org/10.1007/s00442-004-1585-4

Adams, H. D., Zeppel, M. J. B., Anderegg, W. R. L., Hartmann, H., Landhäusser, S. M., Tissue, D. T., Huxman, T. E., Hudson, P. J., Franz, T. E., Allen, C. D., Anderegg, L. D. L., Barron-Gafford, G. A., Beerling, D. J., Breshears, D. D., Brodribb, T. J., Bugmann, H., Cobb, R. C., Collins, A. D., Dickman, L. T., … McDowell, N. G. (2017). A multi-species synthesis of physiological mechanisms in drought-induced tree mortality. *Nature Ecology & Evolution*, *1*(9), 1285–1291. https://doi.org/10.1038/s41559-017-0248-x

Allen, C. D., Breshears, D. D., & McDowell, N. G. (2015). On underestimation of global vulnerability to tree mortality and forest die-off from hotter drought in the Anthropocene. *Ecosphere*, *6*(8), art129. https://doi.org/10.1890/ES15-00203.1

Bacon, J. M. (2019). Settler colonialism as eco-social structure and the production of colonial ecological violence. *Environmental Sociology*, *5*(1), 59–69. https://doi.org/10.1080/23251042.2018.1474725

Baker, K. V., Tai, X., Miller, M. L., & Johnson, D. M. (2019). Six co-occurring conifer species in northern Idaho exhibit a continuum of hydraulic strategies during an

extreme drought year. *AoB Plants*, *11*(5), plz056. https://doi.org/10.1093/aobpla/plz056

Baldy, C. R. (2013). Why we gather: Traditional gathering in native northwest California and the future of bio-cultural sovereignty. *Ecological Processes*, *2*(1), 17. https://doi.org/10.1186/2192-1709-2-17

Barber, V. A., Juday, G. P., & Finney, B. P. (2000). Reduced growth of Alaskan white spruce in the twentieth century from temperature-induced drought stress. *Nature*, *405*(6787), 668–673. https://doi.org/10.1038/35015049

Bennett, A. C., McDowell, N. G., Allen, C. D., & Anderson-Teixeira, K. J. (2015). Larger trees suffer most during drought in forests worldwide. *Nature Plants*, *1*(10), 1–5. https://doi.org/10.1038/nplants.2015.139

Biondi, F., & Qeadan, F. (2008). A theory-driven approach to tree-ring standardization: Defining the biological trend from expected basal area increment. *Tree-Ring Research*, *64*(2), 81–96. https://doi.org/10.3959/2008-6.1

Bohner, T., & Diez, J. (2021). Tree resistance and recovery from drought mediated by multiple abiotic and biotic processes across large geographic gradient. *Science of The Total Environment*, 147744. https://doi.org/10.1016/j.scitotenv.2021.147744

Bond, B. J., & Kavanagh, K. L. (1999). Stomatal behavior of four woody species in relation to leaf-specific hydraulic conductance and threshold water potential. *Tree Physiology*, *19*(8), 503–510.

Borella, S., Leuenberger, M., Saurer, M., & Siegwolf, R. (1998). Reducing uncertainties in $\delta^{13}C$ analysis of tree rings: Pooling, milling, and cellulose extraction. *Journal of Geophysical Research: Atmospheres*, *103*(D16), 19519–19526. https://doi.org/10.1029/98JD01169

Bost, D. S. (2018). Assessing spatio-temporal patterns of forest decline across a diverse landscape in the Klamath Mountains using a 28-year Landsat time-series analysis [Humboldt State University]. https://digitalcommons.humboldt.edu/etd/239/

Bottero, A., D'Amato, A. W., Palik, B. J., Bradford, J. B., Fraver, S., Battaglia, M. A., & Asherin, L. A. (2017). Density-dependent vulnerability of forest ecosystems to drought. *Journal of Applied Ecology*, *54*(6), 1605–1614. https://doi.org/10.1111/1365-2664.12847

Bunn, A., Korpela, M., Biondi, F., Campelo, F., Mérian, P., Qeadan, F., Zang, C., Buras, A., Cecile, J., & Mudelsee, M. (2018). DplR: Dendrochronology program library in R.

Caldeira, M. C., Lecomte, X., David, T. S., Pinto, J. G., Bugalho, M. N., & Werner, C. (2015). Synergy of extreme drought and shrub invasion reduce ecosystem functioning and resilience in water-limited climates. *Scientific Reports*, *5*(1), 15110. https://doi.org/10.1038/srep15110

Campbell, E. M., & Antos, J. A. (2000). Distribution and severity of white pine blister rust and mountain pine beetle on whitebark pine in British Columbia. Canadian Journal of Forest Research, 30(7), 1051–1059. https://doi.org/10.1139/x00-020

Canham, C. D., LePage, P. T., & Coates, K. D. (2004). A neighborhood analysis of canopy tree competition: Effects of shading versus crowding. *Canadian Journal of Forest Research*, *34*(4), 778–787. https://doi.org/10.1139/x03-232

Carnwath, G. C., & Nelson, C. R. (2016). The effect of competition on responses to drought and interannual climate variability of a dominant conifer tree of western North America. *Journal of Ecology*, *104*(5), 1421–1431. https://doi.org/10.1111/1365-2745.12604

Chauvin, T., Cochard, H., Segura, V., & Rozenberg, P. (2019). Native-source climate determines the Douglas-fir potential of adaptation to drought. *Forest Ecology and Management*, *444*, 9–20. https://doi.org/10.1016/j.foreco.2019.03.054

Cleland, D. T., Freeouf, J. A., Keys, J. E., Nowacki, G. J., Carpenter, C. A., & McNab, W. H. (2007). Ecological Subregions: Sections and Subsections for the conterminous United States. In *General Technical Report WO-76D* (Vol. 76D). https://www.fs.usda.gov/treesearch/pubs/48672

Cook, B. I., Ault, T. R., & Smerdon, J. E. (2015). Unprecedented 21st century drought risk in the American Southwest and Central Plains. *Science Advances*, *1*(1), e1400082. https://doi.org/10.1126/sciadv.1400082

Cowan, J. (2019, June 19) “It’s Called Genocide:” Newsom Apologizes to the State’s Native Americans.” *The New York Times.* https://www.nytimes.com/2019/06/19/us/newsom-native-american-apology.html

Crockett, J. L., & Westerling, A. L. (2017). Greater temperature and precipitation extremes intensify western U.S. droughts, wildfire severity, and Sierra Nevada tree mortality. *Journal of Climate*, *31*(1), 341–354. https://doi.org/10.1175/JCLI-D-17-0254.1

Das, A. (2012). The effect of size and competition on tree growth rate in old-growth coniferous forests. *Canadian Journal of Forest Research*, *42*(11), 1983–1995. https://doi.org/10.1139/x2012-142

Dawson, T. E. (1996). Determining water use by trees and forests from isotopic, energy balance and transpiration analyses: The roles of tree size and hydraulic lift. *Tree Physiology*, *16*(1–2), 263–272.

DeCourten, F. (2009). *Custom Enrichment Module; Geology of Northern California*. Cengage Learning. https://books.google.com/books?id=NiltmwEACAAJ

DellaSala, D. A., Reid, S. B., Frest, T. J., Strittholt, J. R., & Olson, D. M. (1999). A global perspective on the biodiversity of the Klamath-Siskiyou ecoregion. *Natural Areas Journal*, *19*(4), 300–319. https://www.jstor.org/stable/43911860

DeSiervo, M. H., Jules, E. S., Bost, D. S., De Stigter, E. L., & Butz, R. J. (2018). Patterns and drivers of recent tree mortality in diverse conifer forests of the Klamath

mountains, California. *Forest Science*, *64*(4), 371–382. https://doi.org/10.1093/forsci/fxx022

DeSoto, L., Cailleret, M., Sterck, F., Jansen, S., Kramer, K., Robert, E. M., Aakala, T., Amoroso, M. M., Bigler, C., & Camarero, J. J. (2020). Low growth resilience to drought is related to future mortality risk in trees. *Nature Communications*, *11*(1), 1–9. https://doi.org/10.1038/s41467-020-14300-5

Dickman, L. T., McDowell, N. G., Sevanto, S., Pangle, R. E., & Pockman, W. T. (2015). Carbohydrate dynamics and mortality in a piñon-juniper woodland under three future precipitation scenarios. *Plant, Cell & Environment*, *38*(4), 729–739. https://doi.org/10.1111/pce.12441

Diffenbaugh, N. S., Swain, D. L., & Touma, D. (2015). Anthropogenic warming has increased drought risk in California. *Proceedings of the National Academy of Sciences*, *112*(13), 3931–3936. https://doi.org/10.1073/pnas.1422385112

Dong, C., MacDonald, G. M., Willis, K., Gillespie, T. W., Okin, G. S., & Williams, A. P. (2019). Vegetation responses to 2012–2016 drought in northern and southern California. Geophysical Research Letters, 46(7), 3810–3821. https://doi.org/10.1029/2019GL082137

Doughty, C. E., Malhi, Y., Araujo-Murakami, A., Metcalfe, D. B., Silva-Espejo, J. E., Arroyo, L., Heredia, J. P., Pardo-Toledo, E., Mendizabal, L. M., Rojas-Landivar, V. D., Vega-Martinez, M., Flores-Valencia, M., Sibler-Rivero, R., Moreno-Vare,

L., Viscarra, L. J., Chuviru-Castro, T., Osinaga-Becerra, M., & Ledezma, R. (2014). Allocation trade-offs dominate the response of tropical forest growth to seasonal and interannual drought. *Ecology*, *95*(8), 2192–2201. https://doi.org/10.1890/13-1507.1

Duursma, R. A., Barton, C. V., Eamus, D., Medlyn, B. E., Ellsworth, D. S., Forster, M. A., Tissue, D. T., Linder, S., & McMurtrie, R. E. (2011). Rooting depth explains CO_2 × drought interaction in *Eucalyptus saligna*. *Tree Physiology*, *31*(9), 922–931. https://doi.org/10.1093/treephys/tpr030

Eziz, A., Yan, Z., Tian, D., Han, W., Tang, Z., & Fang, J. (2017). Drought effect on plant biomass allocation: A meta-analysis. *Ecology and Evolution*, *7*(24), 11002–11010. https://doi.org/10.1002/ece3.3630

Farquhar, G. D., Ehleringer, J. R., & Hubick, K. T. (1989). Carbon isotope discrimination and photosynthesis. *Annual Review of Plant Biology*, *40*(1), 503–537. https://doi.org/10.1146/annurev.pp.40.060189.002443

Fenelon, J. V., & Trafzer, C. E. (2014). From colonialism to denial of California genocide to misrepresentations: Special issue on indigenous struggles in the Americas. *American Behavioral Scientist*, *58*(1), 3–29. https://doi.org/10.1177/0002764213495045

Ferrell, G. T., Otrosina, W. J., & DeMars, C. J. (1994). Predicting susceptibility of white fir during a drought-associated outbreak of the fir engraver, *Scolytus centralis*, in

California. *Canadian Journal of Forest Research, 24*, 301-305. https://doi.org/10.1139/x94-043

Fettig, C. J., Klepzig, K. D., Billings, R. F., Munson, A. S., Nebeker, T. E., Negrón, J. F., & Nowak, J. T. (2007). The effectiveness of vegetation management practices for prevention and control of bark beetle infestations in coniferous forests of the western and southern United States. *Forest Ecology and Management*, *238*(1–3), 24–53. https://doi.org/10.1016/j.foreco.2006.10.011

Gessler, A., Cailleret, M., Joseph, J., Schönbeck, L., Schaub, M., Lehmann, M., Treydte, K., Rigling, A., Timofeeva, G., & Saurer, M. (2018). Drought induced tree mortality–a tree-ring isotope based conceptual model to assess mechanisms and predispositions. *New Phytologist*, *219*(2), 485–490. https://doi.org/10.1111/nph.15154

Gillerot, L., Forrester, D. I., Bottero, A., Rigling, A., & Lévesque, M. (2021). Tree neighbourhood diversity has negligible effects on drought resilience of European beech, silver fir and Norway spruce. *Ecosystems*, *24*(1), 20–36. https://doi.org/10.1007/ s10021-020-00501-y

Goulden, M. L., & Bales, R. C. (2019). California forest die-off linked to multi-year deep soil drying in 2012–2015 drought. Nature Geoscience, 12(8), 632–637. https://doi.org/10.1038/s41561-019-0388-5

Grantham, T. (2018). *North Coast Summary Report* (California's Fourth Climate Change Assessment, p. 80).

Griffin, D., & Anchukaitis, K. J. (2014). How unusual is the 2012–2014 California drought? *Geophysical Research Letters*, *41*(24), 9017–9023. https://doi.org/10.1002/2014GL062433

Griffin, J. R. (1976). *The Distribution of Forest Trees in California*. Pacific Southwest Forest and Range Experiment Station.

Grote, R., Gessler, A., Hommel, R., Poschenrieder, W., & Priesack, E. (2016). Importance of tree height and social position for drought-related stress on tree growth and mortality. *Trees*, *30*(5), 1467–1482.

Hegyi, F. (1974). A simulation model for managing jack-pine stands. Growth models for tree and stand simulation *30*, 74–90.

Holmes, R. L. (1984). Computer-assisted quality control in tree-ring dating and measurement. *Tree-Ring Bulletin*, *43*, 51–67.

Hothorn, T., & Bretz, F. (2008). Simultaneous inference in general parametric models. *Biometrical Journal*, *50*(3), 346–363. https://doi.org/10.1002/bimj.200810425

Hubbard, R. M., Ryan, M. G., Stiller, V., & Sperry, J. S. (2001). Stomatal conductance and photosynthesis vary linearly with plant hydraulic conductance in ponderosa pine. *Plant, Cell & Environment*, *24*(1), 113–121. https://doi.org/10.1046/j.1365-3040.2001.00660.x

Hudiburg, T., Law, B., Turner, D. P., Campbell, J., Donato, D., & Duane, M. (2009). Carbon dynamics of Oregon and northern California forests and potential land-based carbon storage. *Ecological Applications*, *19*(1), 163–180. https://doi.org/10.1890/07-2006.1

Hultine, K. R., & Marshall, J. D. (2000). Altitude trends in conifer leaf morphology and stable carbon isotope composition. Oecologia, 123(1), 32–40.

Iberle, B. G., Van Pelt, R., & Sillett, S. C. (2020). Development of mature second-growth *Sequoia sempervirens* forests. *Forest Ecology and Management*, *459*, 117816. https://doi.org/10.1016/j.foreco.2019.117816

Isaac-Renton, M., Montwé, D., Hamann, A., Spiecker, H., Cherubini, P., & Treydte, K. (2018). Northern forest tree populations are physiologically maladapted to drought. *Nature Communications*, *9*(1), 5254. https://doi.org/10.1038/s41467-018-07701-0

Jackson, G. E., Irvine, J., & Grace, J. (1995). Xylem cavitation in Scots pine and Sitka spruce saplings during water stress. *Tree Physiology*, *15*(12), 783–790. https://doi.org/10.1093/treephys/15.12.783

Kane, J. M., & Kolb, T. E. (2010). Importance of resin ducts in reducing ponderosa pine mortality from bark beetle attack. *Oecologia*, *164*(3), 601–609. https://doi.org/10.1007/s00442-010-1683-4

Kannenberg, S. A., Novick, K. A., & Phillips, R. P. (2018). Coarse roots prevent declines in whole-tree non-structural carbohydrate pools during drought in an isohydric and an anisohydric species. *Tree Physiology*, *38*(4), 582–590.

Kauffmann, M. (2012). *Conifer Country: A natural history and hiking guide to 35 conifers of the Klamath Mountain region*. Backcountry Press.

Keeling, C. D., Piper, S. C., Bacastow, R. B., Wahlen, M., Whorf, T. P., Heimann, M., & Meijer, H. A. (2005). Atmospheric CO_2 and $^{13}CO_2$ exchange with the terrestrial biosphere and oceans from 1978 to 2000: Observations and carbon cycle implications. In A History of Atmospheric CO_2 and its Effects on Plants, Animals, and Ecosystems (pp. 83–113). Springer.

Klein, T. (2014). The variability of stomatal sensitivity to leaf water potential across tree species indicates a continuum between isohydric and anisohydric behaviours. *Functional Ecology*, *28*(6), 1313–1320.

Klein, T., Cohen, S., & Yakir, D. (2011). Hydraulic adjustments underlying drought resistance of *Pinus halepensis*. *Tree Physiology*, *31*, 637–648. https://doi.org/10.1093/treephys/tpr047

Knapp, E. E., Skinner, C. N., North, M. P., & Estes, B. L. (2013). Long-term overstory and understory change following logging and fire exclusion in a Sierra Nevada mixed-conifer forest. *Forest Ecology and Management*, *310*, 903–914.

Lenth, R. (2021). *emmeans: Estimated Marginal Means, aka Least-Squares Means.* (1.5.4.) [R]. https://CRAN.R-project.org/package=emmeans

Level III ecoregions of the continental United States. (2013). [Map]. U.S. Environmental Protection Agency. https://www.epa.gov/eco-research/level-iii-and-iv-ecoregions-continental-united-states

Lévesque, M., Saurer, M., Siegwolf, R., Eilmann, B., Brang, P., Bugmann, H., & Rigling, A. (2013). Drought response of five conifer species under contrasting water availability suggests high vulnerability of Norway spruce and European larch. *Global Change Biology*, *19*(10), 3184–3199. https://doi.org/10.1111/gcb.12268

Linares, J., Delgado-Huertas, A., Camarero, J., Merino, J., & Carreira, J. A. (2009). Competition and drought limit the response of water-use efficiency to rising atmospheric carbon dioxide in the Mediterranean fir *Abies pinsapo*. *Oecologia*, *161*(3), 611–624. https://doi.org/10.1007/s00442-009-1409-7

Linares, J., & Tiscar, P. (2010). Climate change impacts and vulnerability of the southern populations of *Pinus nigra* subsp. *salzmannii*. *Tree Physiology*, *30*(7), 795–806. https://doi.org/10.1093/treephys/tpq052

Magnani, F., Grace, J., & Borghetti, M. (2002). Adjustment of tree structure in response to the environment under hydraulic constraints. *Functional Ecology*, *16*(3), 385–393. https://doi.org/10.1046/j.1365-2435.2002.00630.x

Martínez-Vilalta, J., Sala, A., Asensio, D., Galiano, L., Hoch, G., Palacio, S., Piper, F. I., & Lloret, F. (2016). Dynamics of non-structural carbohydrates in terrestrial plants: A global synthesis. *Ecological Monographs*, *86*(4), 495–516. https://doi.org/10.1002/ecm.1231

Martínez-Vilalta, J., Sala, A., & Piñol, J. (2004). The hydraulic architecture of Pinaceae – a review. *Plant Ecology (Formerly Vegetatio)*, *171*(1/2), 3–13. https://doi.org/10.1023/B:VEGE.0000029378.87169.b1

Mastrandrea, M. D., & Luers, A. L. (2012). Climate change in California: Scenarios and approaches for adaptation. *Climatic Change*, *111*(1), 5–16. https://doi.org/10.1007/s10584-011-0240-4

McCarroll, D., & Loader, N. J. (2004). Stable isotopes in tree rings. *Quaternary Science Reviews*, *23*(7–8), 771–801. https://doi.org/10.1016/j.quascirev.2003.06.017

McCune, B., & Keon, D. (2002). Equations for potential annual direct incident radiation and heat load. *Journal of Vegetation Science*, *13*(4), 603–606. https://doi.org/10.1111/j.1654-1103.2002.tb02087.x

McDowell, N., Brooks, J. R., Fitzgerald, S. A., & Bond, B. J. (2003). Carbon isotope discrimination and growth response of old *Pinus ponderosa* trees to stand density reductions. *Plant, Cell & Environment*, *26*(4), 631–644. https://doi.org/10.1046/j.1365-3040.2003.00999.x

McDowell, N. G., Allen, C. D., & Marshall, L. (2010). Growth, carbon-isotope discrimination, and drought-associated mortality across a *Pinus ponderosa* elevational transect. *Global Change Biology*, *16*(1), 399–415. https://doi.org/10.1111/j.1365-2486.2009.01994.x

McIver, C. P., Meek, J. P., Scudder, M. G., Sorenson, C. B., Morgan, T. A., & Christensen, G. A. (2015). *California's Forest Products Industry and Timber Harvest, 2012* (General Technical Report No. 908; p. 58). US Forest Service.

Meier, I. C., & Leuschner, C. (2008). Belowground drought response of European beech: Fine root biomass and carbon partitioning in 14 mature stands across a precipitation gradient. *Global Change Biology*, *14*(9), 2081–2095. https://doi.org/10.1111/j.1365-2486.2008.01634.x

Monleon, V. J., & Lintz, H. E. (2015). Evidence of tree species' range shifts in a complex landscape. *PLoS One*, *10*(1), e0118069. https://doi.org/10.1371/journal.pone.0118069

Morin, X., & Chuine, I. (2006). Niche breadth, competitive strength and range size of tree species: A trade-off based framework to understand species distribution. *Ecology Letters*, *9*(2), 185–195. https://doi.org/10.1111/j.1461-0248.2005.00864.x

Naficy, C., Sala, A., Keeling, E. G., Graham, J., & DeLuca, T. H. (2010). Interactive effects of historical logging and fire exclusion on ponderosa pine forest structure

in the northern Rockies. *Ecological Applications*, *20*(7), 1851–1864. https://doi.org/10.1890/09-0217.1

Nardini, A., Lo Gullo, M. A., & Salleo, S. (2011). Refilling embolized xylem conduits: Is it a matter of phloem unloading? *Plant Science*, *180*(4), 604–611. https://doi.org/10.1016/j.plantsci.2010.12.011

Nemani, R. R., Keeling, C. D., Hashimoto, H., Jolly, W. M., Piper, S. C., Tucker, C. J., Myneni, R. B., & Running, S. W. (2003). Climate-driven increases in global terrestrial net primary production from 1982 to 1999. *Science*, *300*(5625), 1560–1563. https://doi.org/10.1126/science.1082750

Niinemets, Ü., & Valladares, F. (2006). Tolerance to shade, drought, and waterlogging of temperate northern hemisphere trees and shrubs. *Ecological Monographs*, *76*(4), 521–547. https://doi.org/10.1890/0012-9615(2006)076[0521:ttsdaw]2.0.CO;2

Norgaard, K. M. (2014). Karuk traditional ecological knowledge and the need for knowledge sovereignty: Social, cultural and economic impacts of denied access to traditional management. Report prepared for the Karuk Tribe Department of Natural Resources, Happy Camp, CA.

Norman, S. P., & Taylor, A. H. (2005). Pine forest expansion along a forest-meadow ecotone in northeastern California, USA. *Forest Ecology and Management*, *215*(1), 51–68. https://doi.org/10.1016/j.foreco.2005.05.003

Northern California Indian Development Council. (2021). NCIDC. https://www.ncidc.org/California_Indian_Pre-Contact_Tribal_Territories

Oberhuber, W., Swidrak, I., Pirkebner, D., & Gruber, A. (2011). Temporal dynamics of nonstructural carbohydrates and xylem growth in *Pinus sylvestris* exposed to drought. *Canadian Journal of Forest Research*, *41*(8), 1590–1597. https://doi.org/10.1139/x11-084

O'Hara, K. L., Leonard, L. P., & Keyes, C. R. (2012). Variable-density thinning and a marking paradox: Comparing prescription protocols to attain stand variability in coast redwood. Western Journal of Applied Forestry, 27(3), 143–149. https://doi.org/10.5849/wjaf.11-042

Orwig, D. A., & Abrams, M. D. (1997). Variation in radial growth responses to drought among species, site, and canopy strata. *Trees*, *11*(8), 474–484. https://doi.org/10.1007/s004680050110

Parker, T. J., Clancy, K. M., & Mathiasen, R. L. (2006). Interactions among fire, insects and pathogens in coniferous forests of the interior western United States and Canada. *Agricultural and Forest Entomology*, *8*(3), 167–189. https://doi.org/10.1111/j.1461-9563.2006.00305.x

Peguero-Pina, J. J., Mendoza-Herrer, Ó., Gil-Pelegrín, E., & Sancho-Knapik, D. (2018). Cavitation limits the recovery of gas exchange after severe drought stress in holm oak (*Quercus ilex* L.). *Forests*, *9*(8), 443. https://doi.org/10.3390/f9080443

Pinheiro, J., Bates, D., DebRoy, S., & Sarkar, D. (2018). R Core Team. nlme: Linear and nonlinear mixed effects models.

Pivovaroff, A. L., Cook, V. M. W., & Santiago, L. S. (2018). Stomatal behaviour and stem xylem traits are coordinated for woody plant species under exceptional drought conditions. *Plant, Cell & Environment*, *41*(11), 2617–2626. https://doi.org/10.1111/pce.13367

Pompa-García, M., González-Cásares, M., Acosta-Hernández, A. C., Camarero, J. J., & Rodríguez-Catón, M. (2017). Drought influence over radial growth of Mexican conifers inhabiting mesic and xeric sites. *Forests*, *8*(5), 175. https://doi.org/10.3390/f8050175

Primicia, I., Camarero, J. J., Janda, P., Čada, V., Morrissey, R. C., Trotsiuk, V., Bače, R., Teodosiu, M., & Svoboda, M. (2015). Age, competition, disturbance and elevation effects on tree and stand growth response of primary *Picea abies* forest to climate. *Forest Ecology and Management*, *354*, 77–86. https://doi.org/10.1016/j.foreco.2015.06.034

QGIS Development Team. (2021). *QGIS Geographic Information System*. Open Source Geospatial Foundation Project. http://qgis.osgeo.org

Redmond, M. D., & Barger, N. N. (2013). Tree regeneration following drought-and insect-induced mortality in piñon–juniper woodlands. *New Phytologist*, *200*(2), 402–412. https://doi.org/10.1111/nph.12366

Riikonen, J., Kettunen, N., Gritsevich, M., Hakala, T., Särkkä, L., & Tahvonen, R. (2016). Growth and development of Norway spruce and Scots pine seedlings under different light spectra. *Environmental and Experimental Botany*, *121*, 112–120. https://doi.org/10.1016/j.envexpbot.2015.06.006

Ringgaard, R., Herbst, M., & Friborg, T. (2012). Partitioning of forest evapotranspiration: The impact of edge effects and canopy structure. *Agricultural and Forest Meteorology*, *166*, 86–97. https://doi.org/10.1016/j.agrformet.2012.07.001

Rueda, M., Godoy, O., & Hawkins, B. A. (2017). Spatial and evolutionary parallelism between shade and drought tolerance explains the distributions of conifers in the conterminous United States. *Global Ecology and Biogeography*, *26*(1), 31–42. https://doi.org/10.1111/geb.12511

Sala, A., Woodruff, D. R., & Meinzer, F. C. (2012). Carbon dynamics in trees: Feast or famine? *Tree Physiology*, *32*(6), 764–775. https://doi.org/10.1093/treephys/tpr143

Schoettle, A. W., & Rochelle, S. G. (2000). Morphological variation of *Pinus flexilis* (Pinaceae), a bird-dispersed pine, across a range of elevations. American Journal of Botany, 87(12), 1797–1806. https://doi.org/10.2307/2656832

Schook, D. M., Friedman, J. M., Stricker, C. A., Csank, A. Z., & Cooper, D. J. (2020). Short- and long-term responses of riparian cottonwoods (*Populus* spp.) to flow diversion: Analysis of tree-ring radial growth and stable carbon isotopes. *Science*

of The Total Environment, *735*, 139523. https://doi.org/10.1016/j.scitotenv.2020.139523

Schwarz, P. A., Fahey, T. J., & Dawson, T. E. (1997). Seasonal air and soil temperature effects on photosynthesis in red spruce (*Picea rubens*) saplings. Tree Physiology, 17(3), 187–194. https://doi.org/10.1093/treephys/17.3.187

Schwarz, J. A., Skiadaresis, G., Kohler, M., Kunz, J., Schnabel, F., Vitali, V., & Bauhus, J. (2020). Quantifying growth responses of trees to drought–a critique of commonly used resilience indices and recommendations for future studies. *Current Forestry Reports*, *6*, 185–200. https://doi.org/10.1007/s40725-020-00119-2

Skinner, C. N., & Taylor, A. H. (2006). Southern Cascades bioregion. In N. Sugihara (Ed.), *Fire in California's Ecosystems* (pp. 195–224). University of California Press. https://doi.org/10.1525/california/9780520246058.003.0010

Skinner, C. N., Taylor, A. H., & Agee, J. K. (2006). Klamath Mountains bioregion. In N. Sugihara (Ed.), *Fire in California's Ecosystems* (pp. 170–194). University of California Press. https://doi.org/10.1525/california/9780520246058.003.0009

Slack, A., Kane, J., Knapp, E., & Sherriff, R. (2017). Contrasting impacts of climate and competition on large sugar pine growth and defense in a fire-excluded forest of the central Sierra Nevada. Forests, 8(7), 244. https://doi.org/10.3390/f8070244

Slatyer, R. A., Hirst, M., & Sexton, J. P. (2013). Niche breadth predicts geographical range size: A general ecological pattern. *Ecology Letters*, *16*(8), 1104–1114. https://doi.org/10.1111/ele.12140

Sohn, J. A., Gebhardt, T., Ammer, C., Bauhus, J., Häberle, K.-H., Matyssek, R., & Grams, T. E. (2013). Mitigation of drought by thinning: Short-term and long-term effects on growth and physiological performance of Norway spruce (*Picea abies*). *Forest Ecology and Management*, *308*, 188–197. https://doi.org/10.1016/j.foreco.2013.07.048

Soland, K. R., Kerhoulas, L. P., Kerhoulas, N. J., & Teraoka, J. R. (2021). Second-growth redwood forest responses to restoration treatments. Forest Ecology and Management, 496, 119370. https://doi.org/10.1016/j.foreco.2021.119370

Sthultz, C. M., Gehring, C. A., & Whitham, T. G. (2007). Shifts from competition to facilitation between a foundation tree and a pioneer shrub across spatial and temporal scales in a semiarid woodland. *New Phytologist*, *173*(1), 135–145. https://doi.org/10.1111/j.1469-8137.2006.01915.x

Swain, D. L., Langenbrunner, B., Neelin, J. D., & Hall, A. (2018). Increasing precipitation volatility in twenty-first-century California. Nature Climate Change, 8(5), 427–433. https://doi.org/10.1038/s41558-018-0140-y

Taylor, A. H. (2000). Fire regimes and forest changes in mid and upper montane forests of the southern Cascades, Lassen Volcanic National Park, California, USA.

Journal of Biogeography, 27(1), 87–104. https://doi.org/10.1046/j.1365-2699.2000.00353.x

Taylor, A. H., & Guarin, A. (2005). Drought triggered tree mortality in mixed conifer forests. *In Yosemite National Park*, 229–244. https://doi.org/10.1016/j.foreco.2005.07.014

Teraoka, J. R., & Keyes, C. R. (2011). Low thinning as a forest restoration tool at Redwood National Park. Western Journal of Applied Forestry, 26(2), 91–93. https://doi.org/10.1093/wjaf/26.2.91

Thornburgh, D. (1990). *Picea breweriana* Wats. Brewer spruce. RM Burns and BH Honkala [Tech. Coords.], Silvics of North America, 1, 181–186.

Torregrosa, A., Combs, C., & Peters, J. (2016). GOES-derived fog and low cloud indices for coastal north and central California ecological analyses. *Earth and Space Science, 3*(2), 46–67. https://doi.org/10.1002/2015EA000119

Trifilò, P., Casolo, V., Raimondo, F., Petrussa, E., Boscutti, F., Lo Gullo, M. A., & Nardini, A. (2017). Effects of prolonged drought on stem non-structural carbohydrates content and post-drought hydraulic recovery in *Laurus nobilis* L.: The possible link between carbon starvation and hydraulic failure. *Plant Physiology and Biochemistry, 120*, 232–241. https://doi.org/10.1016/j.plaphy.2017.10.003

Trugman, A. T., Detto, M., Bartlett, M. K., Medvigy, D., Anderegg, W. R. L., Schwalm, C., Schaffer, B., & Pacala, S. W. (2018). Tree carbon allocation explains forest drought-kill and recovery patterns. *Ecology Letters*, *21*(10), 1552–1560. https://doi.org/10.1111/ele.13136

Urban, J., Ingwers, M., McGuire, M. A., & Teskey, R. O. (2017). Stomatal conductance increases with rising temperature. Plant Signaling & Behavior, 12(8), e1356534. https://doi.org/10.1080/15592324.2017.1356534

Urban, O., Klem, K., Ač, A., Havránková, K., Holišová, P., Navrátil, M., Zitová, M., Kozlová, K., Pokorný, R., Šprtová, M., Tomášková, I., Špunda, V., & Grace, J. (2012). Impact of clear and cloudy sky conditions on the vertical distribution of photosynthetic CO_2 uptake within a spruce canopy. *Functional Ecology*, *26*(1), 46–55. https://doi.org/10.1111/j.1365-2435.2011.01934.x

Vernon, M. J., Sherriff, R. L., van Mantgem, P., & Kane, J. M. (2018). Thinning, tree-growth, and resistance to multi-year drought in a mixed-conifer forest of northern California. *Forest Ecology and Management*, *422*, 190–198. https://doi.org/10.1016/j.foreco.2018.03.043

Waring, R. H., Emmingham, W. H., & Running, S. W. (1975). Environmental limits of an endemic spruce, *Picea breweriana*. *Canadian Journal of Botany*, *53*(15), 1599–1613. https://doi.org/10.1139/b75-189

White, J. W. C., & Vaughn, B. H. (2011). Stable isotopic composition of atmospheric carbon dioxide (^{13}C and ^{18}O) from the NOAA ESRL carbon cycle cooperative global air sampling network, 1900-2010. *University of Colorado, Institute of Arctic and Alpine Research*. ftp://ftp.cmdl.noaa.gov/ccg/co2c13/flask/event/

Young, D. J. N., Stevens, J. T., Earles, J. M., Moore, J., Ellis, A., Jirka, A. L., & Latimer, A. M. (2017). Long-term climate and competition explain forest mortality patterns under extreme drought. *Ecology Letters*, *20*(1), 78–86. https://doi.org/10.1111/ele.12711

Zas, R., Sampedro, L., Solla, A., Vivas, M., Lombardero, M. J., Alía, R., & Rozas, V. (2020). Dendroecology in common gardens: Population differentiation and plasticity in resistance, recovery and resilience to extreme drought events in *Pinus pinaster*. *Agricultural and Forest Meteorology*, *291*, 108060. https://doi.org/10.1016/j.agrformet.2020.108060

Zhou, Y., Schaub, M., Shi, L., Guo, Z., Fan, A., Yan, C., Wang, X., Wang, C., Han, S.-J., & Li, M.-H. (2012). Non-linear response of stomata in *Pinus koraiensis* to tree age and elevation. Trees, 26(4), 1389–1396. https://doi.org/10.1007/s00468-012-0713-8

Appendix A

Appendix A: Supplementary tables

Table A1. Summary of mean (± 1 SE) 30-year precipitation from 1981 – 2010 (30-yr Avg) for each precipitation category (dry, moderate, and wet) across sites for each species.

Species	Type	30-yr Avg (mm)
Coastal		
Sitka spruce	Dry	1086 ± 6
	Moderate	1321 ± 25
	Wet	1659 ± 153
Western hemlock	Dry	1132 ± 22
	Moderate	1366 ± 28
	Wet	1743 ± 118
Montane		
Shasta fir	Dry	1294 ± 14
	Moderate	1646 ± 50
	Wet	2405 ± 547
Brewer spruce	Dry	1473 ± 205
	Moderate	1822 ± 95
	Wet	3286 ± 113
Sugar pine	Dry	1044 ± 66
	Moderate	1683 ± 23
	Wet	2801 ± 401
Western white pine	Dry	1248 ± 105
	Moderate	1595 ± 68
	Wet	2682 ± 25

Table A2. Summary of mean (± 1 SE) 30-year precipitation from 1981 – 2010 (30-yr Avg) and mean annual precipitation from 2007 – 2016 (Annual) across sites for each species.

Species	**30-yr Avg (mm)**	**Annual (mm)**
Coastal		
Sitka spruce	1358 ± 60	1327 ± 37
Western hemlock	1468 ± 69	1405 ± 41
Montane		
Shasta fir	1820 ± 168	1111 ± 32
Brewer spruce	2082 ± 217	1352 ± 37
Sugar pine	1816 ± 228	1249 ± 42
Western white pine	1804 ± 149	1129 ± 30

Appendix B

Appendix B: Species-level drought resistance

Isotope-based drought resistance in Sitka spruce and western hemlock was similar and only varied significantly in 2015 (Figure C1 and Figure C2). Both species also experienced a significant rebound in $\Delta^{13}C$ in 2016. Growth-based drought resistance varied between coastal species. In Sitka spruce, growth-based drought resistance decreased from 1.01 (2013) to 0.75 (2014) with no significant change through 2016 (with a resilience value of 0.79). In contrast, growth-based drought resistance in western hemlock decreased from 0.97 (2013) to 0.58 (2016).

Shasta fir, Brewer spruce, sugar pine, and western white pine exhibited little variation in isotope- and growth-based drought resistance with a few exceptions. All four of the montane species experienced marginal to significant declines in isotope-based drought resistance from 2013 to 2014, with western white pine experiencing the largest decrease (from 1.01 to 0.99, Figure C1 and Figure C2). In 2015, isotope-based resistance was significantly higher in Brewer spruce (1.02), but remained similar among all other species (with sugar pine resistance at 0.99 and Shasta fir and western white pine resistance at 1.00). In contrast, growth-based drought resistance did not vary among years or species except in 2016 when Shasta fir and western white pine experienced significant

declines (from 0.93 to 0.84 in Shasta fir, and from 0.96 to 0.80 in western white pine, Figure C1 and Figure C2).

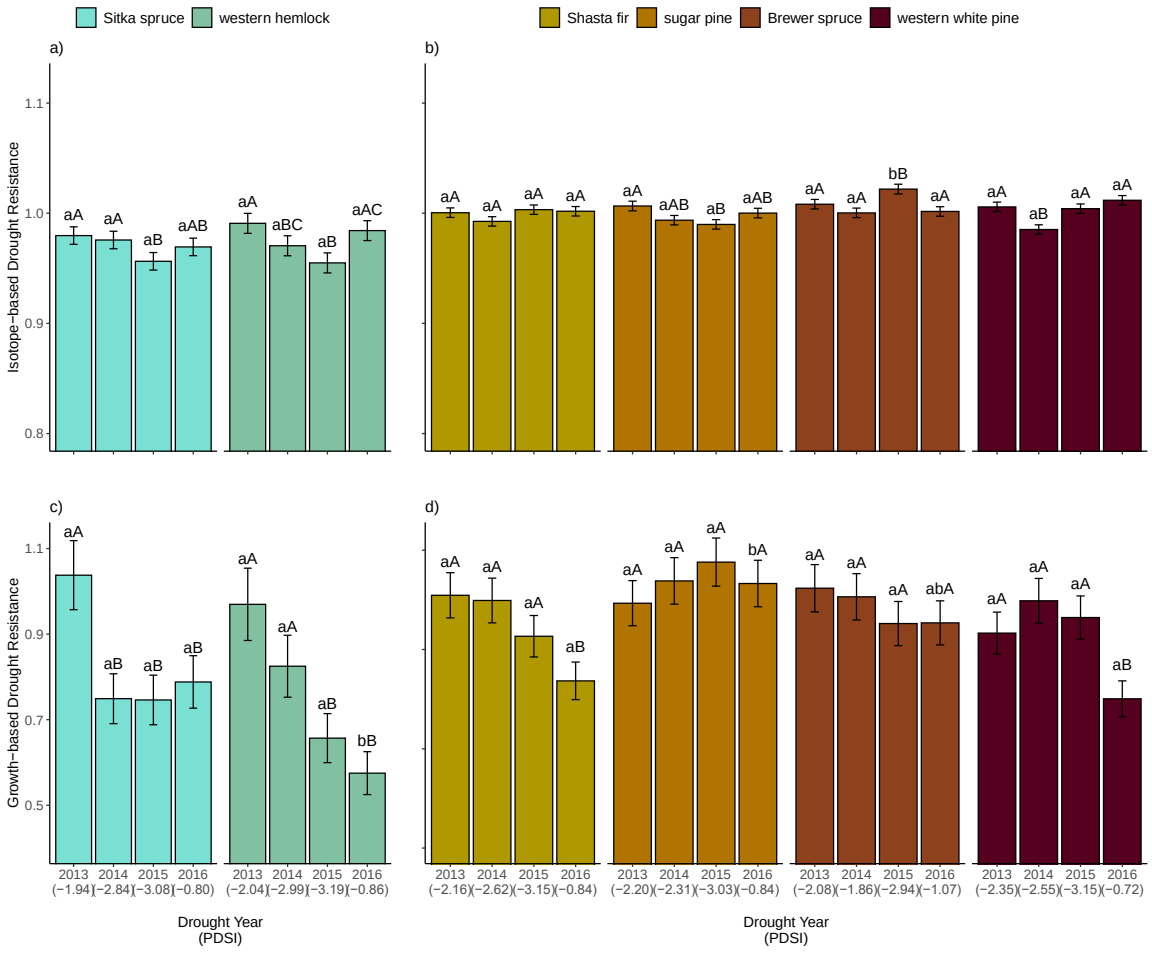

Figure B1. Mean (± SE) annual a) isotope-based drought resistance and b) log of growth-based drought resistance during and after the drought for Sitka spruce and western hemlock (coastal species), and for Shasta fir, Brewer spruce, sugar pine, and western white pine (montane species). Different lowercase letters represent significant ($p < 0.05$) differences among species, while different uppercase letters represent differences among years within species. Note that the y-axis extends from 0.80 to 1.10 in a) and from 0.50 to 1.10 in b).

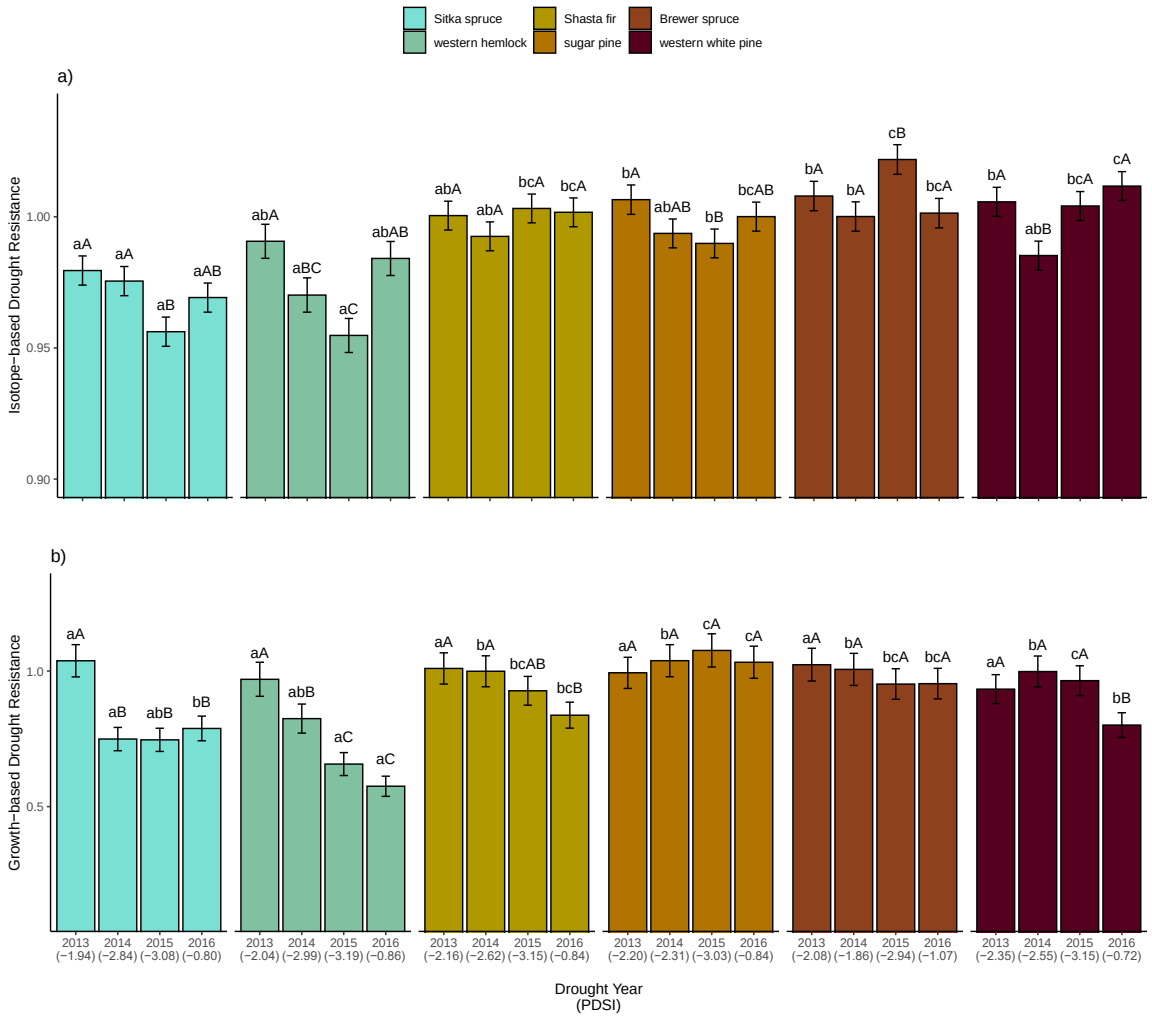

Figure B2. Mean (± SE) annual a) isotope-based drought resistance and b) log of growth-based drought resistance during and after the drought for Sitka spruce and western hemlock (coastal species) and Shasta fir, Brewer spruce, sugar pine, and western white pine (montane species). Different lowercase letters represent significant ($p < 0.05$) differences among species, while different uppercase letters represent differences among years within species. Note that the y-axis extends from 0.80 to 1.10 in a) and from 0.50 to 1.10 in b). Note that the model used to make this figure suffered from high multicollinearity.

Appendix C

Appendix C: Explanatory variables for the $\Delta^{13}C$ models. Each table contains variables for one of the four variable categories.

Table C1. Competition variables for the $\Delta^{13}C$ models.

Covariate	Description	Data Source
Hegyi Index (CI)	Competition index that accounts for diameter and distance between focal and competitor trees (see Equation 5). More competition may reduce moisture availability per tree.	Calculated from field data for each tree based on competitor trees present within a 10 m radius.
Conspecific Hegyi Ratio (CI_{CS})	The proportion of competition that can be attributed to intraspecific competition. More intraspecific competition may reduce moisture and nutrient availability among conspecifics.	Calculated from field data for each tree based on competitor trees present within a 10 m radius.
Trees per Hectare (TPH)	Number of trees present per hectare. More trees per hectare could reduce moisture and nutrient availability, but more trees per hectare may also correspond with smaller trees and different light environments. Small trees have more weight relative to the Hegyi Index.	Calculated from field data for each tree based on competitor trees present within a 10 m radius.

Table C2. Drought and climate variables for the $\Delta^{13}C$ models.

Covariate	Description	Data Source
Annual Water-Year Precipitation (PPT)	Annual precipitation (mm) from the previous year's October through the current year's September. Higher values correspond with more moisture availability.	Summed monthly data from Climatology Lab – TerraClimate
Minimum Temperature (T_{min})	Minimum annual temperature (ºC). Higher values indicate warmer winters and could correspond with a longer growing season as well as less snowpack (stored water) in montane sites.	Minimum from monthly data from Climatology Lab – TerraClimate
Maximum Temperature (T_{max})	Maximum annual temperature (ºC). Higher values indicate warmer dry seasons, and correspond with higher evapotranspirational demand.	Maximum from monthly data from Climatology Lab – TerraClimate
30-Year Average Precipitation (PPT_{30})	Average annual precipitation from 1981 – 2010. Higher values correspond with more historic moisture availability.	PRISM climate data

Table C3. Site characteristic variables for the $\Delta^{13}C$ models.

Covariate	Description	Data Source
Heat Load Index (HLI)	Uses slope, aspect, and latitude to calculate potential direct radiation. Higher values indicate greater light availability but also higher potential evapotranspirational demand.	spatialEco package
Elevation	A measure (m) of elevation above sea level. Higher values generally correspond with more precipitation.	USGS National Elevation Dataset
Serpentine	Binary yes or no variable regarding whether or not the site is on serpentine soil. May affect tree vigor and carbon stores.	USGS Landsat Data

Table C4. Tree characteristic variables for the $\Delta^{13}C$ models.

Covariate	Description	Data Source
Species	Sitka spruce, western hemlock, Shasta fir, Brewer spruce, sugar pine, and western white pine. Different species have different ranges of $\Delta^{13}C$.	Data were collected for 45 focal trees of each tree species
Diameter at Breast Height (DBH)	Tree diameter (cm) at 1.37 m height. Larger trees may be under greater hydraulic stress and/or have deeper root systems and access to different water sources.	Collected in field

Appendix D

Appendix D: Interaction plots for $\Delta^{13}C$ models

Table D1. Range of modeled and actual values for the response and predictor variables presented in the Sitka spruce interaction plot (Figure D1). Variables include ^{13}C discrimination ($\Delta^{13}C$), heat load index (HLI), and water-year precipitation (PPT_{wy}). Predictor variable ranges are listed by standard deviations (SD) away from the mean.

Variable	Model Range	Data Range
$\Delta^{13}C$ (‰)	18.0 to 20.0	15.7 to 24.2
HLI (SD)	-0.5 to +0.5	-1.3 to +1.0
PPT_{wy} (SD)	-1.0 to +1.5	-0.9 to +1.3

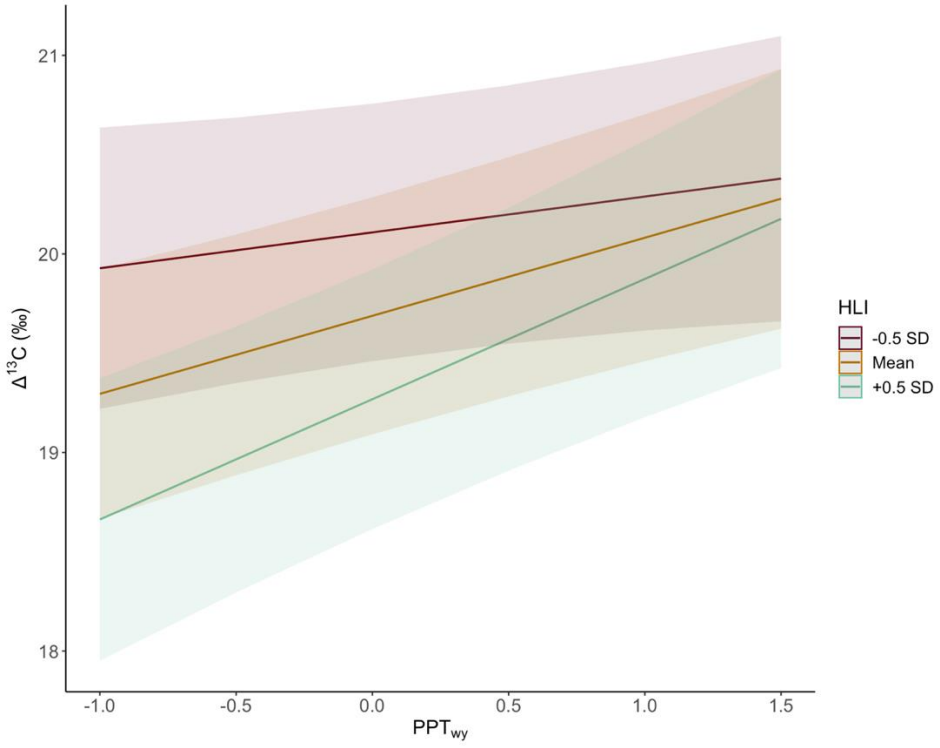

Figure D1. Interaction plots for heat load index (HLI) and water-year precipitation (PPT_{wy}) for the Sitka spruce ^{13}C discrimination ($\Delta^{13}C$) model. Lines represent the model's prediction for trees at sites with HLI at or half a standard deviation away from the mean and shading represents the 95% confidence interval for each line.

Table D2. Range of modeled and actual values for the response and predictor variables presented in the pooled coastal model interaction plot (Figure D2). Variables include ^{13}C discrimination ($\Delta^{13}C$), trees per hectare (TPH), and water-year precipitation (PPT_{wy}). Predictor variable ranges are listed by standard deviations (SD) away from the mean.

Variable	Model Range	Data Range
$\Delta^{13}C$ (‰)	18.0 to 20.0	15.7 to 24.2
TPH (SD)	-0.5 to +0.5	-0.6 to +2.8
PPT_{wy} (SD)	-1.0 to +1.5	-0.9 to +1.3

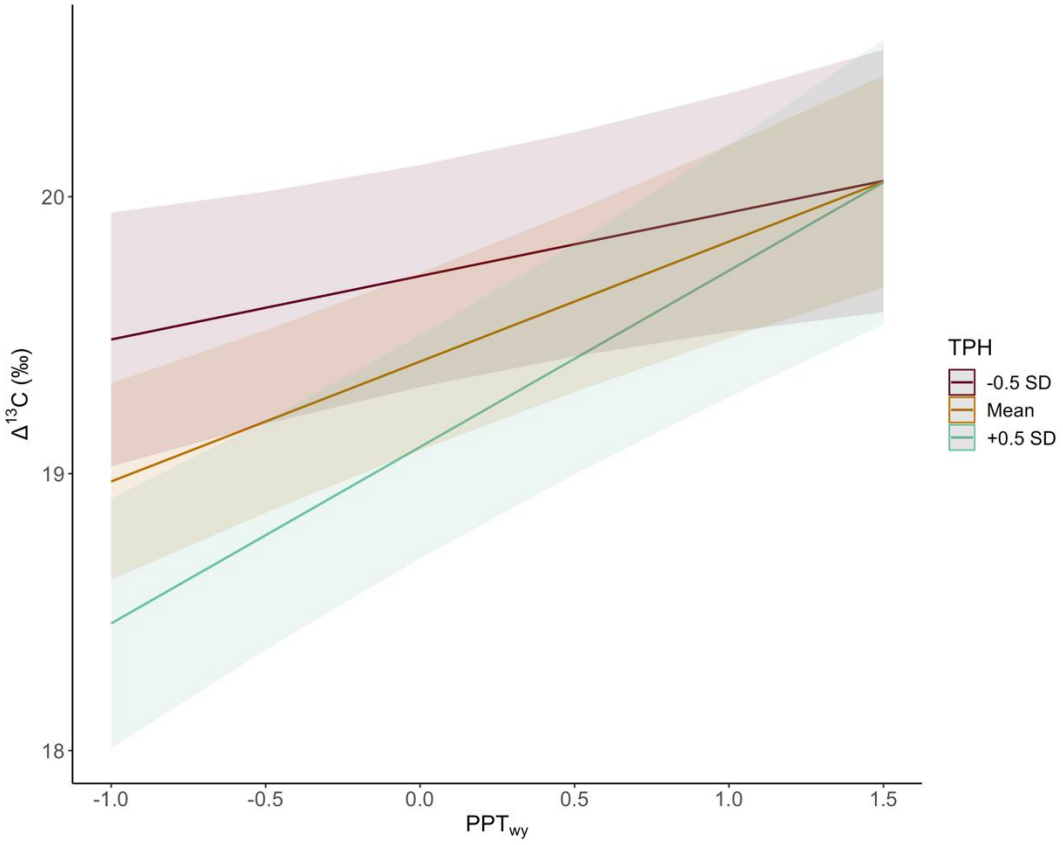

Figure D2. Interaction plots for trees per hectare (TPH) and water-year precipitation (PPT_{wy}) for the pooled coastal ^{13}C discrimination ($\Delta^{13}C$) model. Lines represent the model's prediction for trees with TPH at or half a standard deviation away from the mean and shading represents the 95% confidence interval for each line.

Table D3. Range of modeled and actual values for the response and predictor variables presented in the Shasta fir model interaction plot (Figure D3). Variables include ^{13}C discrimination ($\Delta^{13}C$), diameter at breast height (DBH), and water-year precipitation (PPT_{wy}). Predictor variable ranges are listed by standard deviations (SD) away from the mean.

Variable	Model Range	Data Range
$\Delta^{13}C$ (‰)	17.0 to 19.0	15.4 to 20.7
DBH (SD)	-0.5 to +0.5	-0.9 to +1.3
PPT_{wy} (SD)	-1.0 to +2.0	-0.8 to +1.6

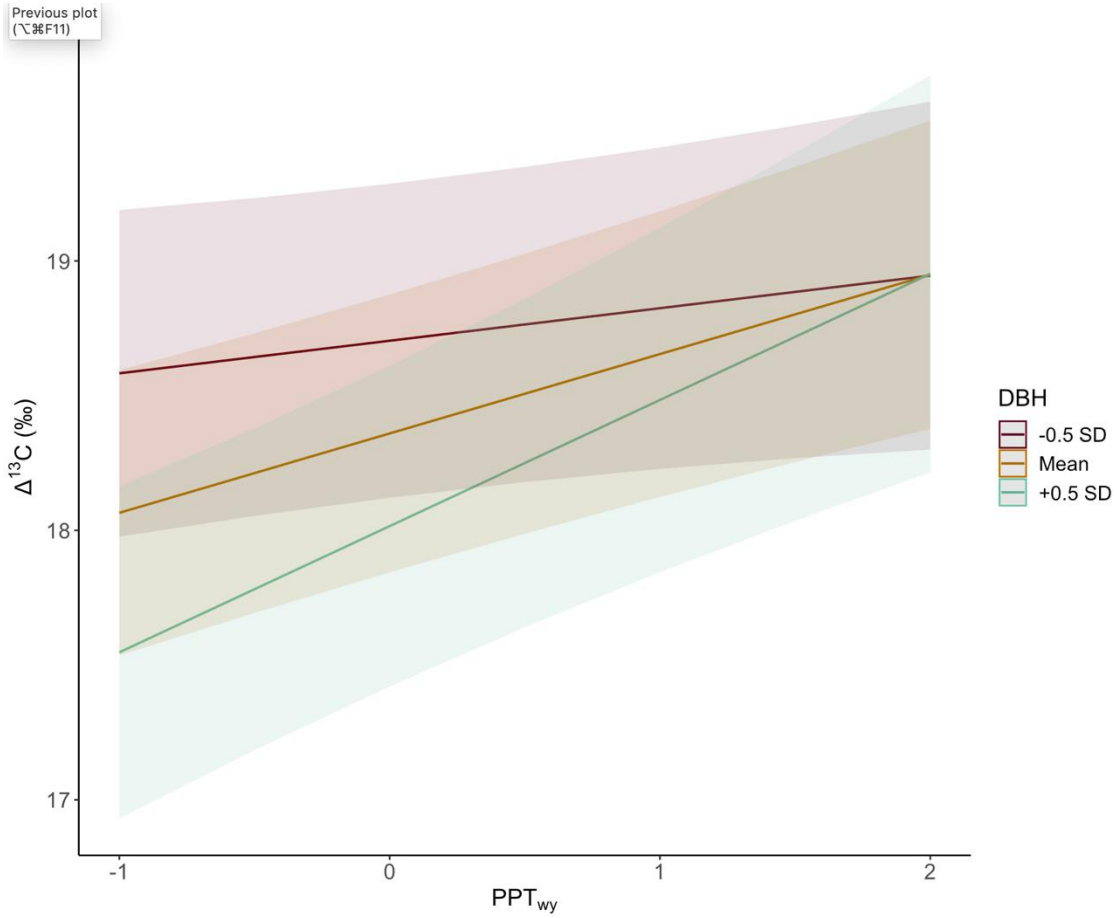

Figure D3. Interaction plot for diameter at breast height (DBH), and water-year precipitation (PPT_{wy}) for the Shasta fir ^{13}C discrimination ($\Delta^{13}C$) model. Lines represent the model's prediction for trees with DBH values at or half a standard deviation away from the mean and shading represents the 95% confidence interval for each line.

Table D4. Range of modeled and actual values for the response and predictor variables presented in the Brewer spruce model interaction plot (Figure D4). Variables include ^{13}C discrimination ($\Delta^{13}C$), annual minimum temperature (T_{min}), and water-year precipitation (PPT_{wy}). Predictor variable ranges are listed by standard deviations (SD) away from the mean.

Variable	Model Range	Data Range
$\Delta^{13}C$ (‰)	16.5 to 17.7	14.8 to 19.6
T_{min} (SD)	-0.5 to +0.5	-1.1 to +0.9
PPT_{wy} (SD)	-1.0 to +1.0	-1.0 to +1.0

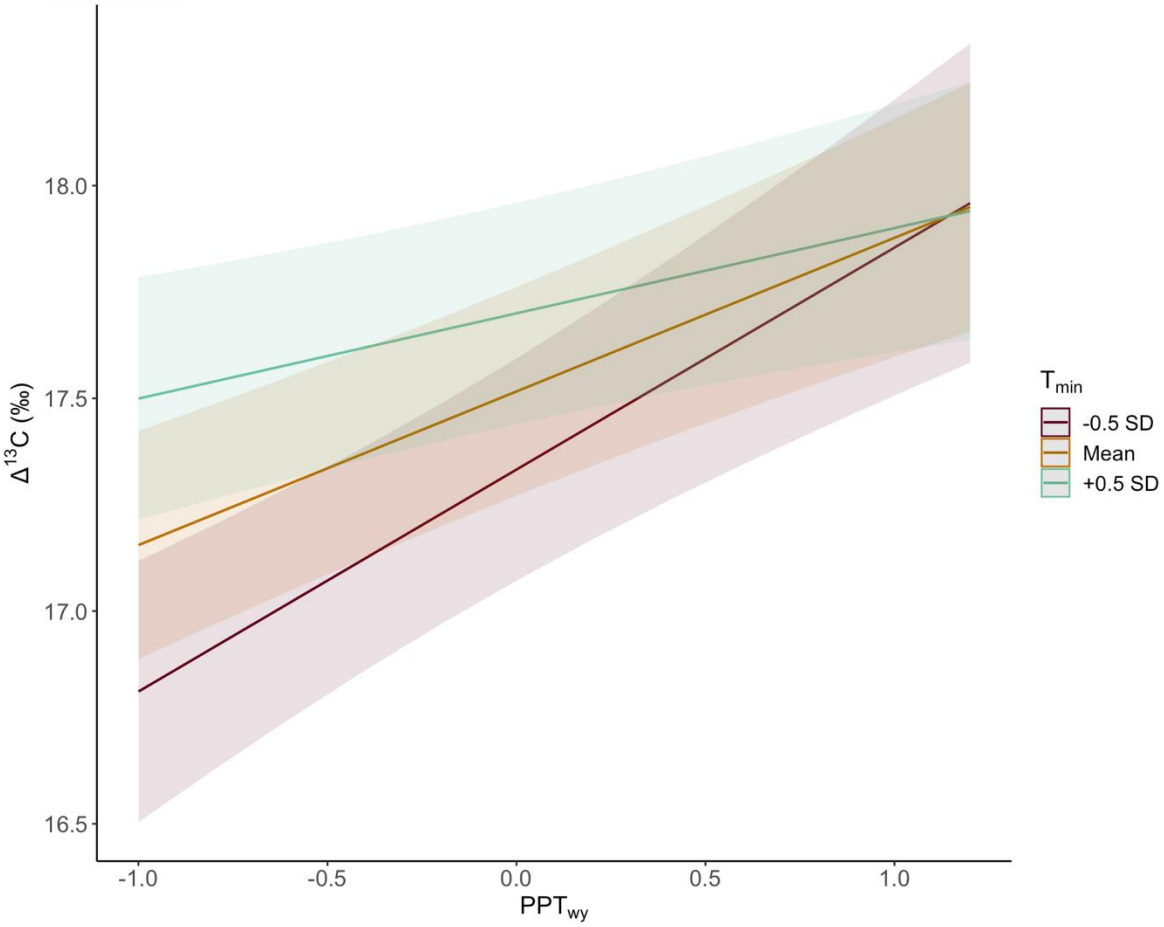

Figure D4. Interaction plot for minimum temperature (T_{min}) and water-year precipitation (PPT_{wy}) for the Brewer spruce ^{13}C discrimination ($\Delta^{13}C$) model. Lines represent the model's prediction for trees at sites with T_{min} at or half a standard deviation away from the mean and shading represents the 95% confidence interval for each line.

Appendix E

Appendix E: Plot of montane pooled model

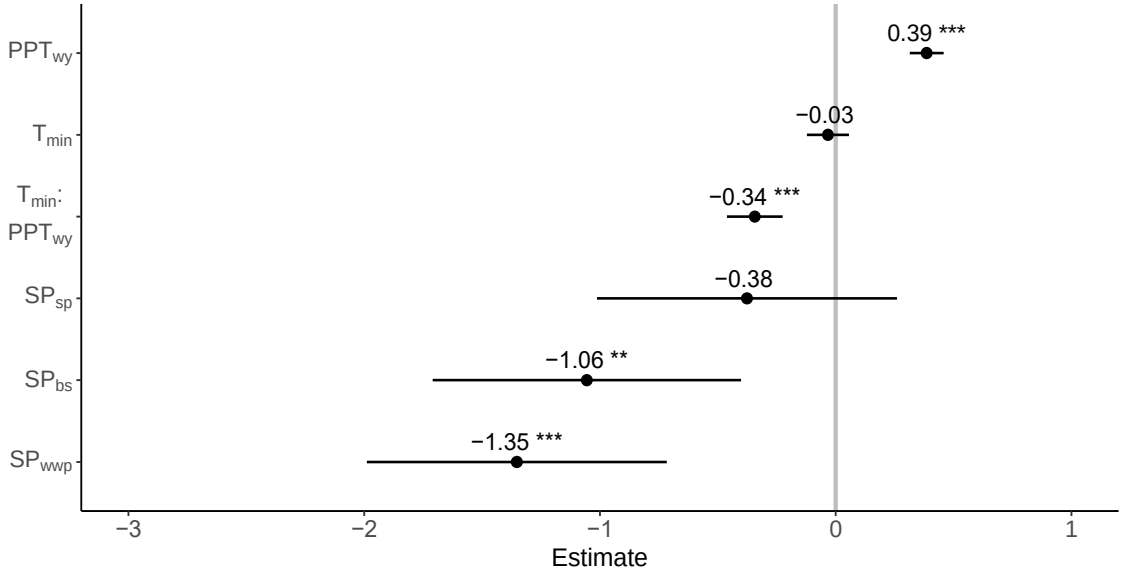

Figure E1. Model estimates with 95% confidence intervals of each predictor variable in the best models for explaining variation in ^{13}C discrimination ($\Delta^{13}C$, years 2007 – 2016) in the montane species pooled (Shasta fir, Brewer spruce, sugar pine, and western white pine, *n* = 1776 tree-rings with 180 trees). Predictor variables include: water-year precipitation (PPT_{wy}), minimum annual temperature (T_{min}), and species effects (SP) for sugar pine, Brewer spruce, and western white pine (sp, bs, and wwp, respectively) relative to the Shasta fir default (intercept, not shown). Asterisks denote significance levels of *p*-values (* < 0.05, ** < 0.01, and *** < 0.001).

Appendix F

Appendix F: Coastal species stand density and species richness across a precipitation gradient

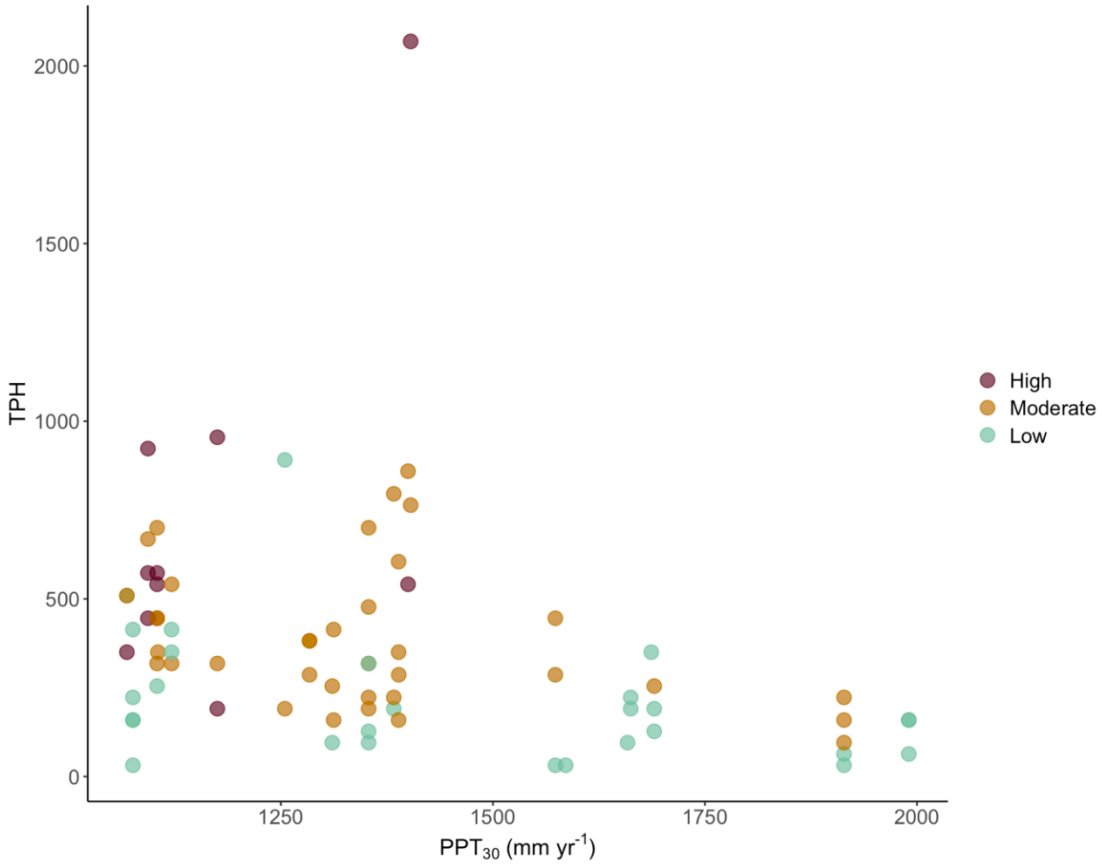

Figure F1. Trees per hectare (TPH) for every tree in the coastal species dataset plotted against 30-year average precipitation (PPT_{30}) values. Point color indicates species richness category, with low (green) indicating a species richness of less than three species per plot, moderate (yellow) indicating species richness of three or four species per plot, and high (red) indicating species richness above four species per plot. Minimum species richness was one and maximum species richness was seven.

Appendix G

Appendix G: $\Delta^{13}C$ and BAI from 2007 to 2016 for wet and dry sites

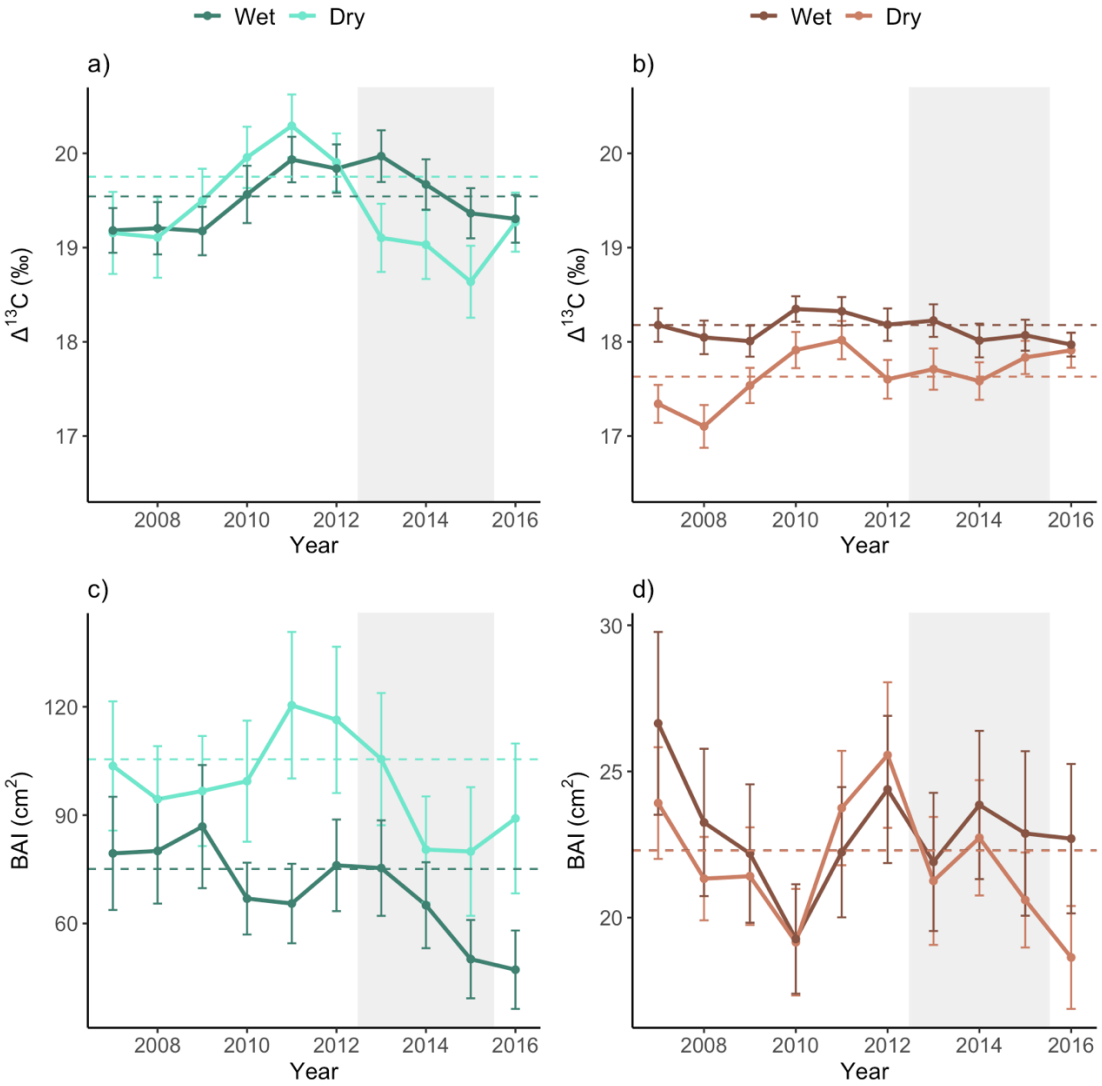

Figure G1. Timeseries for mean (± SE) ^{13}C discrimination ($\Delta^{13}C$, a and b) and annual basal area increment (BAI, c and d) across the study period for wet and dry sites for coastal (a and c) and montane (b and d) species. Grey area represents drought period, and dashed lines indicate pre-drought averages. All sites were located in northern California.

Appendix H

Appendix H: Supplemental species figures

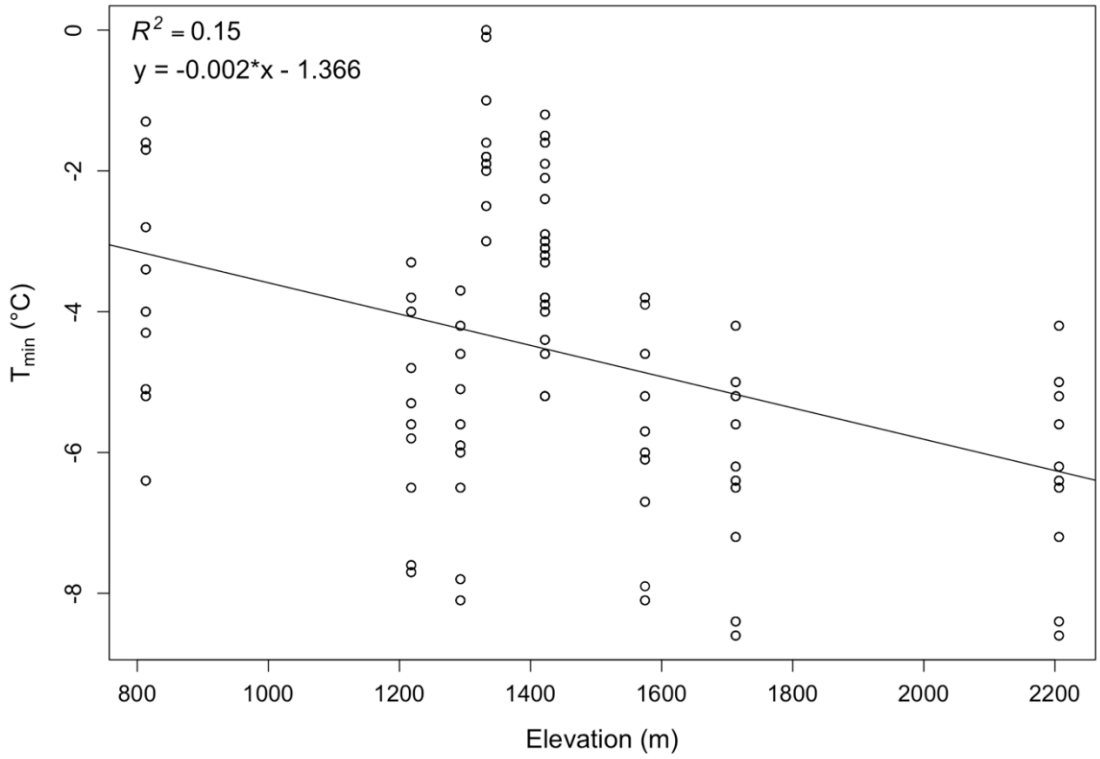

Figure H1. Elevation and minimum annual temperatures (T_{min}) for all sugar pine sites. Black line is the regression line for these data. Multiple $R^2 = 0.15$, $p < 0.001$.

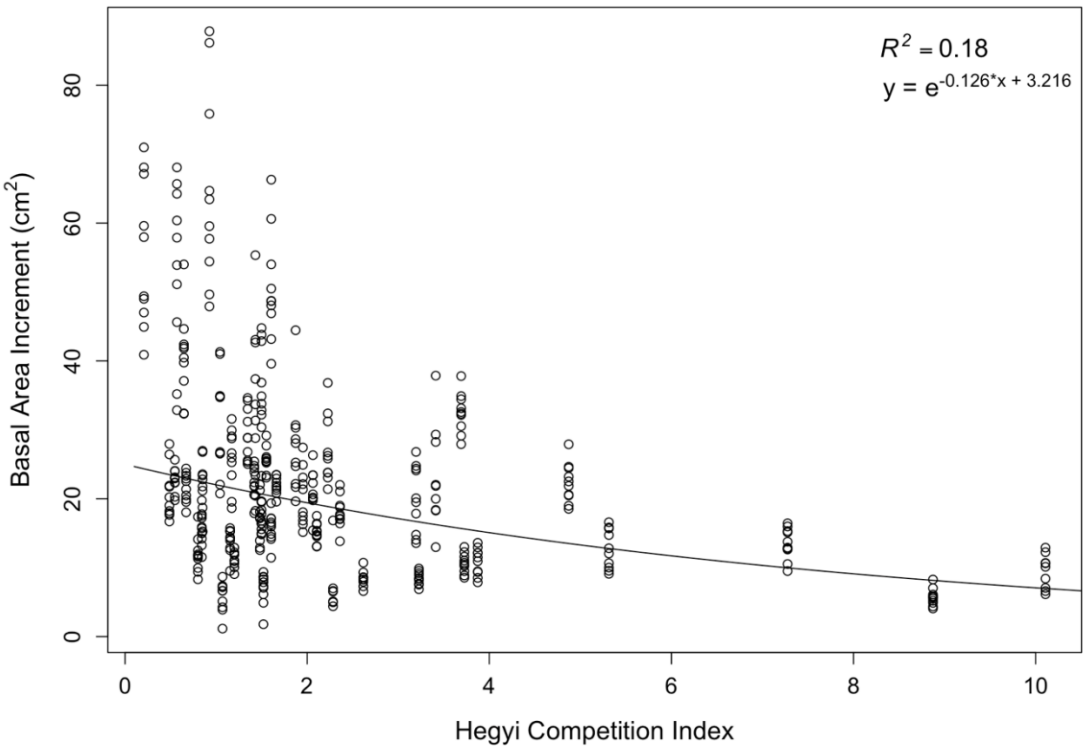

Figure H2. Hegyi index (CI) and basal area increment (BAI) for Brewer spruce. Black line is the back-transformed regression line for these data. Multiple $R^2 = 0.18$, $p < 0.001$.